COMMUNITY ECOLOGY 7(1): 53-67, 2006
1585-8553/$20.00 © Akadémiai Kiadó, Budapest
DOI: 10.1556/ComEc.7.2006.1.6

Multiscale analysis of palynological records: new possibilities

L. Orlóci[1, 2], V. D. Pillar[1] and M. Anand[3,4]

[1] *Departamento de Ecologia, Universidade Federal do Rio Grande do Sul, Porto Alegre, RS, 91540-000, Brazil. E-mail: lorloci@sympatico.ca, vpillar@ecologia.ufrgs.br*
[2] *Permanent address: Department of Biology, The University of Western Ontario, London, N6G 4V1, Canada*
[3] *Department of Biology, Laurentian University, Sudbury, Ontario, P3E 2C6, Canada. Email: Anand.madhur@gmail.com*
[4] *Department of Environmental Biology, University of Guelph, Guelph, Ontario, N1G 2W1, Canada*

Keywords. Acceleration, Composition, Correlogram, Formation, Pattern, Palynology, Spectra, Stability, Statistics, Synchronicity, Temperature, Trajectory, Vegetation, Velocity, Vostok.

Abstract. Palynological records helped to illuminate the past, but we show the take can be made much sharper when statistical analysis recognises the records' scale dependence. The latter is an unavoidable consequence of site selection, sediment sampling, and the samples' arrangement into time series by dating. To make provision for this in statistical analysis, scale has to be incorporated as one of the intrinsic variables. But by incorporating scale, the analysis will render the outcome not to be a single conclusion, the usual case in conventional statistics, but a multitude of conclusions each regarding the same set of response and forcing variables and each as valid at its own scale as any of the other conclusions at theirs. Thus, the central question for a usable Statistics is this: how to incorporate scale into the analysis and still have a unique conclusion. We address the methodological aspects and illustrate them by worked examples. We use 14 sites scattered across the globe. Interestingly, the analysis of these brought forth hitherto hidden aspects of the temporal synchronicity of change in palynological composition and concomitant atmospheric temperature oscillations that should greatly interest Ecology, as one critique put it, in the age of Global Change. The examples testify to a conceptual advance in laying open a very basic principle: the synchronicity's statistically strong formation specificity, dominantly positive (in frequency terms) for climate warming at sites in the currently humid, micro- and mesothermal zones, and negative in the currently arid and semi-arid zones. Our paper begins with an introduction to the terminology of multiscale analysis in Ecology, followed by data sources, the method we call *canonical serial scaling*, and objectives. A detailed discussion of data properties with special attention to error sources in palynology is provided. The method components discussed include the scalars of compositional transition and synchronicity, error dampening, stabilisation of the synchronicity scalar and its sign distribution, analysis of time shifted series, the use of deviation graphs, and pointers to help detect hotspots and other characteristic points of change on the time axis.

One of the greatest pains to human nature is the pain of a new idea.
Walter Bagehot (1969)

Introduction

We present a methodology that we call *canonical serial scaling*. We do not blame the reader for thinking that "canonical" is a misnomer, after an unsuccessful search through dictionaries for a meaningful entry in the statistical context. Yet, the term "canonical" has the right connotation. It indicates the presence of groups (canons, categories) of variables to be subjected to analysis as groups simultaneously and correlatively. Uniquely in what we do, one group contains the response variables (pollen, spore, or cell counts) and the other the forcing (environmental) variables. Again uniquely, both groups have associated intrinsic variables specific to "scale". In the most generic sense we are dealing with scales of pattern and process. In the commonest case the scale is spatial or temporal. It is intuitive to regard the perception of pattern and process as a scale dependent variable, specific to the mode in which these phenomena are observed. This implies accepting as a fact of common experience that the observer sees pattern and process one way on one scale and another way on other scales. The experience conditioning interests has lead early to adoption of a multiscale view of pattern in Ecology. The seminal work of Greig-Smith (1952, 1983) with multiscale ground patterns of vegetation is an

éclat example. As a most general outcome, Greig-Smith defines the ecological paradigm in which "... the causes of patterns of distributions, patterns of all scales …" are the central objects of inquiry. The essence of the point would not change if we substituted time for space in pattern analysis.

The minimum outcome of Greig-Smith's pattern analysis is a series of scale related intensity values (inferences, conclusions) generated by varying the ground scale (block size) at which pattern is observed. The technique thus incorporates "scale" as an intrinsic variable. As a consequence, Greig-Smith's inferences about species pattern and the linkages of species pattern to environmental forcing are scale dependent. So in the analysis the inference itself becomes a scale dependent variable. What is the advantage of making inference a variable? Simply stated, the analysis will allow the practitioner to identify scale points at which pattern or process reach maximum sharpness or the linkage to concomitant environmental forcing attains maximum strength. This way of measuring pattern fits Schneider's (1994) broader definition of "scaling".

The emphasis in vegetation ecology has shifted over the decades from the micro patterns edaphically forced and ruled by competition, which so much interested Greig-Smith, to the mega patterns that challenge current global change research. Reynolds and Wu (1999) dissertate on the latter and its implications. Raising the scale interests us not just out of curiosity, but directly as a context for the objectives that we set, namely, to find regularities in temporal transitions of palynological composition and their synchronicity with changes in high-level environmental forcing. It is on this scale that our work has contact points with current global change research, concerning the climate (Walther et al. 2002; IPCC, 2001) and its destabilizing effects on the vegetation (Samuel et al. 1999).

In short, we subject temporal palynological data to multiscale analysis. There is an entire science about the analysis of this kind of data as time series. Rayner (1971) gives a relatively simple introduction. The most noted of the variants run under such names as harmonic analysis (Wiener 1930), spectral analysis (Wonnacott 1961), time series analysis (Hannan 1960), and spatial analysis (Ripley 1977, 1981). These all have their unique and also shared constraints, the regularity conditions under which their application can be sanctioned. As far as the present case of *canonical serial scaling* is concerned, there is but a single requirement: identifiable common points on the temporal axis. We will discuss or point to specifics in the sequel.

Our primary objective with *canonical serial scaling* is to examine the long-term vegetation process as it enfolded in the past that shaped the current global vegetation pattern. The time scale in our examples reaches back to at least 20 k yr BP, and in one case to almost 200 k yr BP. The palynological records of that era of the late Quaternary were interpreted by palynologists who collected the sediment samples and recorded their contents. There are many facts already known about the broad historic shifts in the global vegetation cover and their timing vis-à-vis the forcing climatic cycles. What then could we offer anew to what is already known? The questions we pose are not about the fact of global shifts, but rather about how closely synchronous were the shifts in palynological composition in the sediment profiles and the peaks and lows in atmospheric temperature oscillations. Our questions touch two major problem areas in quantitative ecology: data acquisition and statistical inference.

Considering data acquisition, we had no control over sampling design or techniques of measurement. All data sets were received from recognised sources[1]. The methodology of data analysis is another matter. With this we could rely on our own results (Orlóci et al. 2002).

The paleoecological record

Before we discuss the records general characteristics, we introduce the sites from which we obtained palynological spectra. The location details, contact person, and other site information are laid out in Table 1. Deuterium based temperature estimates are given in Fig. 1, following Petit et al. (1999).

The palynological record will allow effective targeting of the vegetation process only in the limited terms of compositional transitions. The limits are set by the population level of the identified taxa and the inherent noise-like oscillations in the data. Regarding these, the population level is ill-defined in systematic terms, since the taxa amount to no more in the analysis than paleopollen, spore, or other tissue types. These could correspond to any systematic level, and they do mainly higher than species or genera. The consequence of this is a potentially low ecological resolving power of the analysis.

1 Palynological records were downloaded from the Global Pollen Database (http://www.ncdc.noaa.gov/paleo/ftp-pollen.html) in 2000. One of the record sets is H. Behling's (see Behling et al. 2004). The temperature records were downloaded from the World Data Center for Paleoclimatology (http://www.ngdc.noaa.gov/paleo/icecore/antarctica/vostok) in 2002.

Table 1. Description of palynological spectra used in the case examples. Vegetation classification and precipitation records follow Kühler (1990) and Trewartha (1990). Potential evapotranspiration records follow Trewartha (2001). Legend to symbols: T – Tundra; TR – Tropical rainforest; LSC – Lowland shrub conifer; TA – Taiga; AT – Alpine tundra; TDF – Temperate deciduous forest; ARA – Araucaria forest; TG – Tropical grassland; G – other grassland; XF – Xerophytic forest; TH – Thorn shrub; EAS – Eucalyptus, acacia shrub; EASC – EAS plus Conifer; MDSC – Montane desert shrub conifer; DS – Desert shrub. See addresses to contact persons and data sources in Footnote 1.

Location and contact person	Latitude Longitude Altitude m	Number of taxa Number of time steps	Period covered yr BP	Regional vegetation formation Annual precipitation (cm) Potential evapo- transpiration (cm)
1. Lagoa das Patas, Amazonas – P. E. Oliveira (Colinvaux et al. 1996)	00.16.00N 66.41.00W 300	179 49	0 - 44569	TR >200 120-160
2. Joe Lake, Alaska – P. M. Anderson (1988)	66.46.00N 157.13.00w 183	90 87	0 - 43804	T,TA 25-50 <40
3. Camel Lake, Florida – E.C. Grimm (Watts et al. 1992)	30.16.00N 85.01.00W 20	147 116	0 - 36658	LSC 100-150 80-120
4. Hanging Lake, Yukon Territory – L. C. Cwynar (1982)	68.28N 138.23W 500m	89 133	0 - 41134	T 25-50 <40
5. Jack London Lake, Magadan Oblast, Russia – P. M. Anderson (Lozhkin et al. 1993)	62.10.00N 149.30.00E 820	72 60	221 - 29876	AT,TA 25-50 <40
6. Jackson Pond, Kentucky – G. R. Wilkins (Wilkins et al. 1991)	37.27.00N 85.43.00W 212	71 58	0 - 20477	TDF 100-150 80-120
7. Cambará, Rio Grande do Sul, Brazil – H. Behling (Behling et al. 2004)	29.03.09S 50.06.04W 1046	164 190	0 - 42784	ARA,G 150-200 80-120
8. Lake Patzcuaro, Michoacán de Ocampo, Mexico – W. A. Watts (Watts and Bradbury 1982)	19.35.00N 101.35.00W 2044	53 64	20 - 44100	XF 50-100 120-160
9. Rusaka Swamp, Burundi – R. Bonnefille (Bonnefille et al. 1995)	03.26.00S 29.37.00E 2070	179 141	796 - 11910 (46666)	TG,TH 50-150 120-160
10. Lynch's Crater, Queensland, Australia – A. P. Kershaw (1994)	17.22.00S 145.42.00E 760	22 44 (234)	868 – 40000 (-192649)	EAS 50-150 120-160
11. Harberton, Tierra del Fuego – V. Markgraph (no reference given).	54.53.00S 67.10.00W 20	33 81	0 - 13360	DS 25-50 80-120
12. Lake George, NSW – G. S. Hope (Singh and Geissler 1985)	35.05.00S 149.25.00E 673	93 30 (68)	1 – 40000 (116711)	EASC 25-100 80-120
13. Potato Lake, Arizona – R. S. Anderson (1993)	34.27.43N 111.20.43W 2205	77 61	1389 - 35271	MDSC 25-50 80-160
14. Hay Lake, Arizona – B. F. Jacobs (1985)	34.00.00N 109.25.30W 2780	44 46	106 - 44692	MDSC 25-50 80-160

The noise-like data oscillations can come from a multiplicity of sources (Orlóci et al. 2002). We mention the main ones:

(1) *Broad geographic base.* Pollen, spore, and algal cells can originate outside the site or even beyond the immediate region. What is adding further to the problem is the

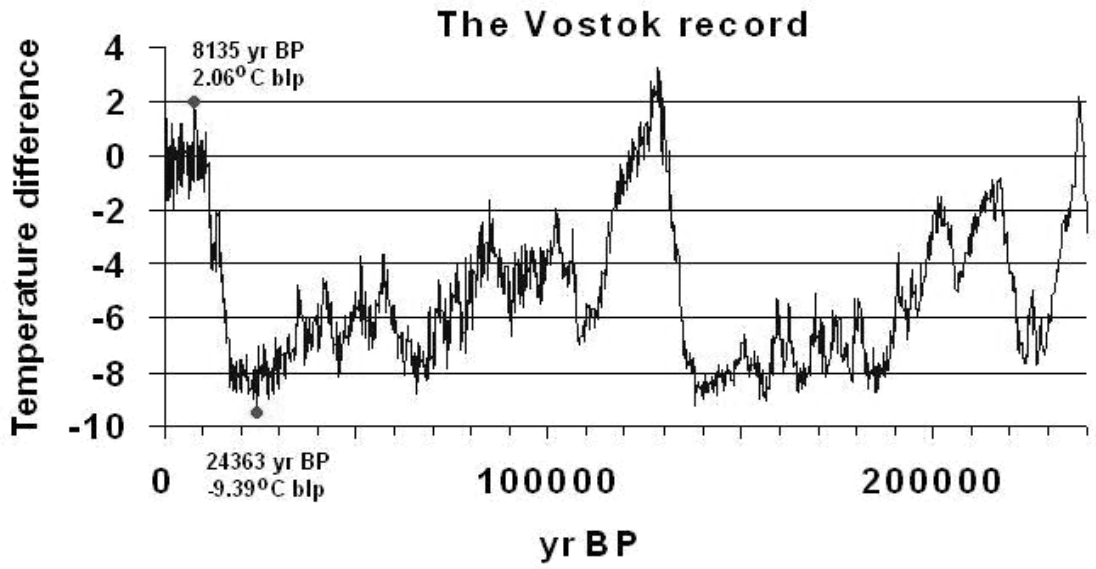

Figure 1. Inversion layer temperature oscillations expressed as differences from present, following Petit et al. (1999). Temperature values are deuterium based from ice core at Vostok, Eastern Antarctic (78° S, 106° E). Zero point on the temperature scale corresponds to the current state of deuterium in the higher atmosphere. See the text, for further details.

common presence of exogenous materials that cannot be separated from the materials originated in the site. These all but rule out inferences of a local nature that will not apply also in the broader geographic area. Charcoal macro particles and other plant remains are the exceptions that may have more definitely local origin.

(2) *Plant type identification.* Pollen, spore, cell, or other plant tissue is identifiable with only limited taxonomic accuracy in most cases. An inevitable consequence of this is the mixing of taxa from different systematic levels in the same sample. This blurs the specificity of statistical inference.

(3) *Site selection, sediment sampling, extraction of organic remains, dating.* Each of these is an error source in itself specific to the technique used and also to the implementation of the techniques. We discuss some implications in the present paper and refer to work by others for additional details and references (Libby 1955, Lowe and Walker 1997, and Orlóci et al. 2002). The reader is referred to the original web files (see footnote 1) regarding the dating method used. The approach is far from being uniform. It involves mostly linear and low order polynomial interpolation between the radiocarbon dates. Linear extrapolation is common, and occasionally the extrapolation is based (dubiously) on polynomials. In at least one case (Cambará) calibration of the radiocarbon dates is available (see Appendix 5, for details). We assumed that in all other cases uncalibrated dates were given, since no "calibration" is mentioned. We used uncalibrated dates in the Cambará sample.

We make a distinction between two main sources for noise-like data oscillations. One includes *chance events* and the other includes *bias*. The chance events have to do with pollen and spore production, transport, sedimentation, preservation, and like events. *Bias* comes as part and parcel of personal choices made when siting sediment cores and locating sediment samples, committing mistakes of a systematic nature in taxon identification, erroneously logging measurements. The chance related noise can be handled as part of the symmetric error terms of variation and controlled by the usual tools of statistical design and analysis. Bias cannot be handled this way. It should be avoided with foresight. We present in this paper a technique for noise dampening when the noise is chance related. The user should keep it in mind that for a whole spectrum of sources the errors may intensify by non-linear feedback in system components' behaviour, the case of the fractal (Orlóci 2001) and accumulate to produce extreme chaotic dynamics (Anand 2000). We do not deal with the problem of measuring that kind of feedback in this paper, but we are confident that the 'scaling' method we present can be extended to handle the problem reasonably well (Orlóci et al. 2002).

Regarding our source for atmospheric temperature records we mention that the choice of Vostok is forced upon us by circumstance. Why did we choose Vostok? The first

thing to be observed about this is the non-existence of other sources to our knowledge for long-term temperature records in the range we specified anywhere in the sites. The choice is thus reduced to one source out of two: Greenland or Vostok. When we tested Vostok, we obtained sensible results. The Greenland record appeared ill-conditioned and did not produce an interpretable outcome. We mention further in support of Vostok, findings in two paleoclimatic and deep ocean studies of Stocker (2000) and Clark et al. (2002). According to these studies, changes in the Polar climates have wide rippling effects in the global atmosphere, possibly with a millennial scale asynchrony for abrupt and delayed warming events in Greenland compared to the Antarctic (Blunier and Brook 2001). We interpret this as being supportive of the global synchronicity hypothesis regarding atmospheric oscillations across the globe, even though the magnitude of oscillations can be different at different sites. Other impressive aspects offering further support to our use of Vostok include the long sampling period and relatively high sampling intensity; the known geographic correlation of deuterium content and temperature in the high atmosphere where precipitation forms (Schweingruber 1996); and the reasonably close reproducibility of Vostok temperature patterns by records taken elsewhere from glacial ice, terrestrial sediments and deep-see deposits (Petit et al. 1999, Stocker 2000). For further details regarding temperature inferences from the isotopic content of ice, and the determination of ice age by the combined ice-flow ice-accumulation model, we refer to Petit et al. (1999) and Lorius et al. (1985).

Method components and numerical examples

With constraints as given, it may appear hopelessly risky to expect much from statistical analysis, if it requires "clean data" that the mathematically "neat" classical statistical techniques stipulate (Orlóci 1993). Fortunately, there are effective ways to ease the constraints and to find answers to such pointed questions as we will phrase concerning the synchronicity of change in palynological composition and in environmental forcing, formation specificity of synchronicity, and the siting of hot spots of change. But, before we can precisely pose these questions, we need to describe the essentials of the methodology.

Compositional transition scalars

$V \mid \frac{d}{\div t}$:average compositional transition velocity over time period $\div t$; always positive; interpretable as average instability in the site's palynological composition.

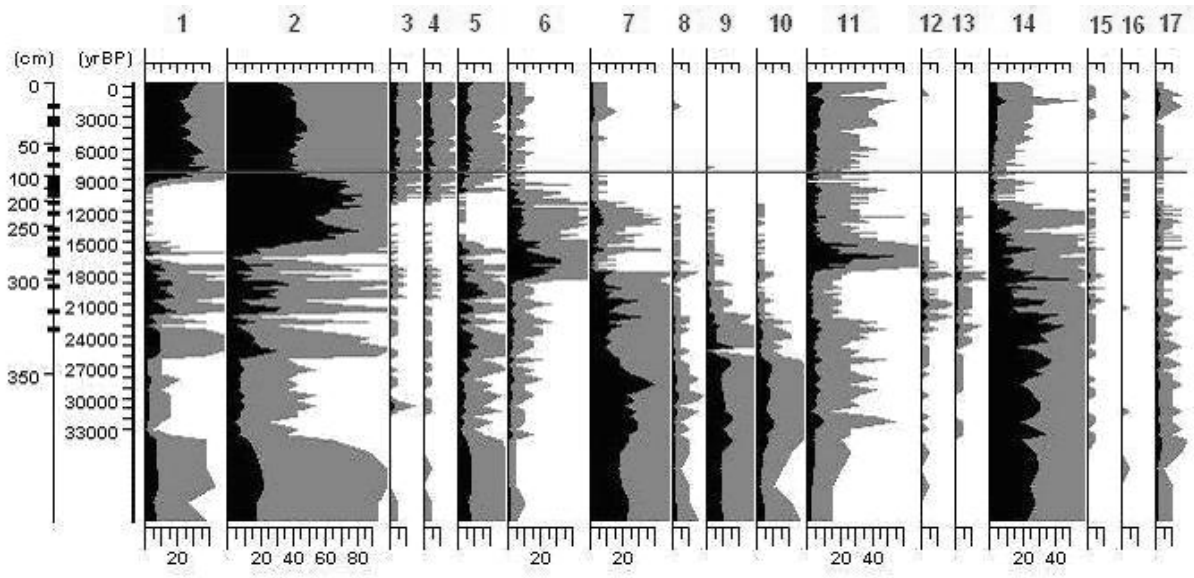

Figure 2. Cwynar's (1982) palynological records from Hanging Lake, Yukon Territory. Sample and location are described in Table 1. Graph and accompanied data were downloaded from the Global Pollen Database (see the main text for web address). Short listed taxa after L.C. Cwynar: 1 *Alnus,* 2 *Betula,* 3 Ericaceae, 4 Ericales, 5 *Picea,* 6 *Salix,* 7 *Artemisia,* 8 Asteraceae-Asteroideae, 9 Brassicaceae, 10 Chenopodiaceae/Amaranthaceae, 11 Cyperaceae, 12 Fabaceae, 13 *Plantago canescens,* 14 Poaceae, 15 Rosaceae, 16 Other trees and shrubs, 17 Other herbs. Bottom scale: pollen counts %. Dark shading: original scale. Light shading: 5Δ exaggerated scale. Black markings on depth scale: dated horizons. Horizontal line inside graph demarks a record set called *paleorelevé*. This is the virtual equivalent of the regional vegetation community 8200 years BP.

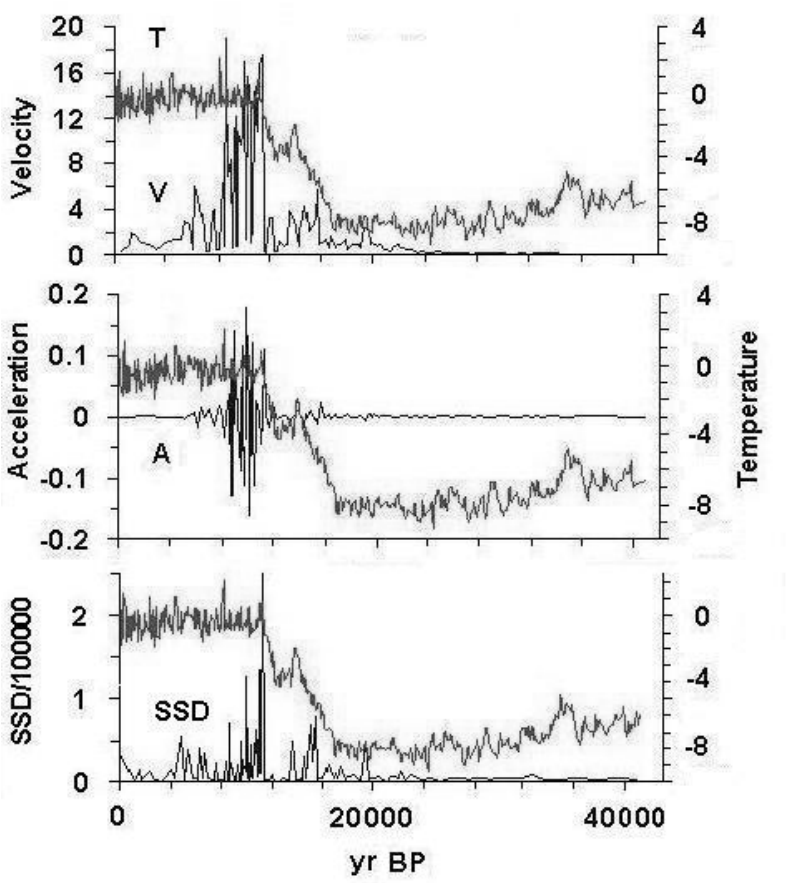

Figure 3. Vostok temperature differences *(T),* compositional transition velocity *(V),* acceleration *(A),* and squared compositional deviation *(SSD)* from random expectation over time (yr BP) for L.C. Cwynar's Hanging Lake record sequence (Fig. 1). Appendix 1 contains the graphs for all sites. Horizontal axis: time before present. Time begins at top sediment horizon. Some details and references are given in the main text. Petit et al. (1999, 2000, 2001) describe details of the temperature records.

d: Euclidean distance of two paleorelevés time units apart. The "paleorelevé" is an ecologist's term for the palynological record-set for a given horizon of the sediment core (horizontal line inside Fig. 2).

$A \mid \frac{V_{t2 \div t} - V_t}{\div t}$: average compositional transition acceleration (when positive) or deceleration (when negative); interpretable as the amount of change in compositional stability over time period $\div t$.

Extreme peaks in the *A* graphs of Fig. 3 and Appendix 1 identify time points of dramatic change in palynological composition. We refer to the extreme peaks as *hotspots of change*.

Synchronicity scalar

$$r(V,T) \mid \frac{\sum_i (V_i - \bar{V})(T_i - \bar{T})}{\sqrt{\sum_i (V_i - \bar{V})^2 \sum_i (T_i - \bar{T})^2}} :$$

as written, a product moment correlation of compositional transition velocity *V* and atmospheric temperature oscillations *T*.

$\bar{V}, \bar{T}$: averages of the entire V,T sequence.

The product moment has its advantages/disadvantages (Orlóci 1978), but if users prefer other synchronicity measures in the –1 to 1 range the analysis can accommodate them. Whatever the case, the *r(V,T)* values are best not to be calculated directly from the original *V* and *T* records of the graphs, but from the adjusted values after error dampening. Our method of error dampening is based on moving averages. The technique is best explained by example as in Table 2.

F^+, F^-: the synchronicity scalar's sign frequency distribution; interpreted as the tendency of *r(V,T)* to be negative or positive under chance ruled sampling of the same *V,T* sequence. For this, the *n–BS*+1 valued time series of running averages is re-sampled by way of randomly laid sub series of random length (minimum 5 and maximum *n-BS*+1 units); a new value of *r(V,T)* is computed for each sub series; and by repeating the process a large number of times the frequencies of negative (F^-) and positive (F^+) *r(V,T)* are found.

The magnitude of *r(V,T)* and the nature of its sign frequency distribution are key characteristic of the palynological process. Strong positive synchronicity is indicated when *r(V,T)* is positive and numerically large.

Table 2. Calculation of moving averages. Block size starts at step size 1, incremented in units of one (on time axis). In general terms, there are *BS* = 1, 2, 3, …, *M*<*n* block sizes and for each block size *n*–*BS*+1 moving averages. We chose not to have an *M* value larger than 40 in long series. In the example above, *n* = 10 and *M* = 4. The extreme right column in the table contains the values of the synchronicity scalar.

Bock size (BS)	Variable	Values of *V* and *T* at time points before present										*r*(*V*,*T*)
		1	2	3	4	5	6	7	8	9	10	
1	*V*	3	3	5	6	6	1	4	8	3	9	0.963
1	*T*	-1	-2	3	4	4	-3	1	5	0	6	
2	*V*	3	4	5.5	6	3.5	2.5	6	5.5	6		0.963
2	*T*	-1.5	0.5	3.5	4	0.5	-1	3	2.5	3		
3	*V*	3.7	4.7	5.7	4.3	3.7	4.3	5	6.7			0.996
3	*T*	0	1.7	3.7	1.7	0.7	1	2	3.7			
4	*V*	4.3	5	4.5	4.3	4.8	4	6				0.934
4	*T*	1	2.2	2	1.5	1.8	0.8	3				

Table 3. Regression estimates and related statistics read off Fig. 4 and Appendix 2. See method and data details in the text. Symbols *V, T, r(V,T),* $\psi(V,T)$, R^2, λ^+, and *BS* are same as in Figs 3-4. Additional symbols: *LL* and *UL* – lower and upper limits of the 95% confidence interval about the regression estimate (normally distributed statistical errors are assumed); Thi – Thornthwaite index (precipitation per potential evapotranspiration); CRVF – current regional vegetation formation; T – Tundra; TR – Tropical rainforest; LSC – Lowland shrub conifer; TA – Taiga; AT – Alpine tundra; TDF – Temperate deciduous forest; ARA – Araucaria forest; G – temperate grassland; TG – Tropical grassland; XF – Xerophytic forest; TH – Thorn shrub; EAS – Eucalyptus, acacia shrub; EASC – EAS plus conifer; MDSC – Montane desert shrub conifer; DS – Desert shrub.

Locality	$\rho(V,T)$	LL	UL	R^2	ϕ^+	ϕ^-	CRVT	Thi
Lagoa das Patas 00.16N 6.41W	0.12	-0.01	0.28	0.73	80.96	16.30	TR	>1.43
Joe Lake 66.46N 157.13W	0.35	0.30	0.40	0.98	80.90	16.76	T	1.88
Camel Lake 30.16N 85.01W	0.31	0.27	0.35	0.98	75.84	20.68	LSC	1.25
Hanging Lake 68.28N 138.23W	0.63	0.56	0.71	0.91	68.68	30.22	T TA	1.88
Jack London L. 62.10N149.30E	0.11	0.02	0.20	0.98	65.08	29.16	AT TA	1.88
Jackson Pond 37.27N 85.43W	0.30	0.28	0.32	0.98	57.31	38.39	TDF	1.25
Cambará 29.03S50.06W	0.53	0.50	0.56	0.95	56.63	32.77	ARA G	1.75
Lake Patzcuaro 19.35N 101.35W	0.60	0.50	0.70	0.78	52.79	41.25	XF G	0.54
Rusaka Swamp 3.25S 29.37E	0.23	0.17	0.24	0.86	46.84	39.99	TG TH	0.71
Lynch's Crater* 17.22S 145.42E	-0.66	-0.70	-0.62	0.74	42.62	55.08	EAS	0.71
Tierra del Fuego 54.53S 67.10W	-0.25	-0.37	-0.15	0.55	33.64	63.71	DS	0.36
Lake George* 35.05S 149.25E	-0.48	-0.99	-0.28	0.57	15.12	84.32	EASC	0.63
Potato Lake 37.27N 111.20W	-0.31	-0.42	-0.19	0.86	11.15	84.91	MDSC	0.31
Hay Lake 34.00N 109.25W	-0.23	-0.34	-0.12	0.85	4.74	93.91	MDSC	0.31
Mean (positive)	0.35	0.29	0.42	0.91	65.00	29.50		1.39
Mean (negative)	-0.39	-0.56	-0.27	0.71	21.45	76.39		0.46
Grand mean	0.09	-0.02	0.17	0.84	49.45	46.25		1.04

Correlation values: $\rho(V,T)$ *x Thi = 0.621;* ϕ^+ *x Thi = 0.821;* ϕ^- *x Thi = -0.804.*

* Current 40 k yr period analysed.

Table 4. Calculations at *Lag* = 0, 1, 2, 3. The basic data come from rows *BS* = 1 in Table 2.

Bock size (BS)	Lag	Variable	Values of V and T at time points before present										r(V,T)
			1	2	3	4	5	6	7	8	9	10	
1	0	V	3	3	5	6	6	1	4	8	3	9	0.963
1		T	-1	-2	3	4	4	-3	1	5	0	6	
1	1	V	3	3	5	6	6	1	4	8	3		-0.186
1		T	-2	3	4	4	-3	1	5	0	6		
1	2	V	3	3	5	6	6	1	4	8			-0.174
1		T	3	4	4	-3	1	5	0	6			
1	3	V	3	3	5	6	6	1	4				0.028
1		T	4	4	-3	1	5	0	6				

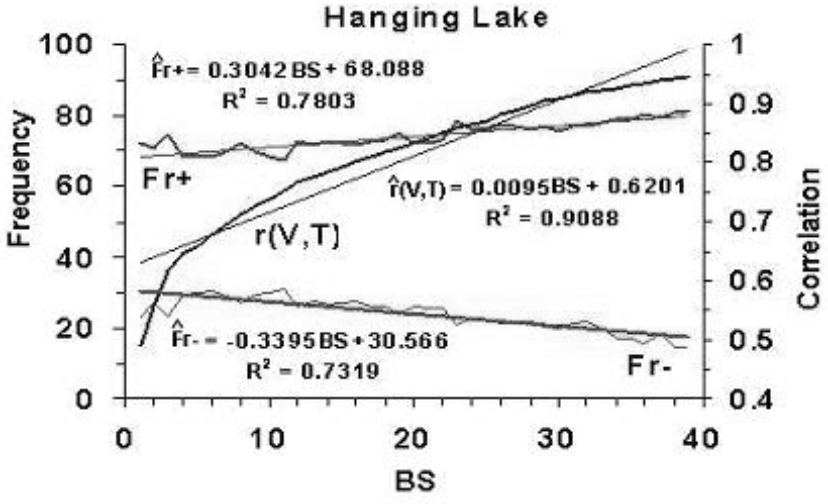

Figure 4. Graphical outline of the regression method for estimation of stable synchronicity and frequency values. Symbols: *V* - compositional transition velocity; *T* - Vostok temperature; *BS* – block size for averages; F^+ and F^- - sign frequencies; *r(V,T)* – synchronicity; R^2 - coefficient of determination; $\psi(V,T) = 0.63$, $\lambda^+ = 68$; $\lambda^- = 30$ – stable estimates at *BS* = 1 based on the regression equations; heavy lines - values derived from moving averages; light lines – fitted regression lines for the equations. See explanations and references in the main text. The numerical results are summarised in Table 3.

Formation specificity is indicated when one of F^+, F^- is dominant (see following explanations).

Stabilisation of the synchronicity scalar and its sign frequencies

A new *r*(*V*,*T*) value is calculated from moving averages at each *BS*. There are *M* new *r(V,T)* values to which we fit line $\hat{r}$ *(V,T) (*see Fig. 4 and Appendix 2). We take *b*+*a,* the regression estimate of the current synchronicity value at *BS*=1, as the "stable" synchronicity estimate ψ(V,T). We do similar calculations with the sign frequencies to obtain the stable estimates λ^+ and λ^-. The sample values are summarised in Table 3.

Determination of λ^+ and λ^- in the time shifted V and T series

Until this point we retained a time equivalent pairing of the *V* and *T* values. Now we pose the question: what will happen to λ^+ and λ^- if we shifted the *T* series forward in time (left in the *V,T* graphs) so that the time lag of the *V* and *T* values paired widens from 0 to 1 then to 2, 3, and so forth in millennial steps. To illustrate this, we take the example of Table 2 and define *Lag* = 0, 1, 2, 3 for *BS = 1* in Table 4. This is done in the same manner to each of the remaining *BS* = 2, 3, 4. At each *Lag*, we re-compute the $\psi(V,T)$, λ^+ and λ^- estimates for *BS* = 1 in the same manner as already described. The basic graphs that result in the Hanging Lake case are in Fig. 5 and all the graphs in Appendix 3. The dominant stable sign frequencies are identified in Table 5.

Deviations from random expectation

$D_{ij} \mid X_{ij} 4\, e_{ij}, SSD_j \mid \underset{i}{\overline{\quad}} D_{ij}^2, e_{ij} \mid \frac{X_{i.}, X_{.j}}{X_{..}}$:

e_{ij} - random expectation, a compositional state that would occur if a chance ruled process were generating pa-

Table 5. Identification of dominant stable sign frequencies at *BS* = 1 of the synchronicity scalar at different *Lag* (thousand year units). See the method description in the text. Dominant λ^+ is indicated by + and dominant λ^- by –. Lag code is Lag/1000. Symbols in bold face identify points at which the dominant sign frequency or correlation change direction considerably (hotspots). Note the robust adherence of the sites to their value at *Lag* = 0 up until about *Lag* = 10 k yr or even longer, except for the transitional cases 8, 9, and unexpectedly 6. Legend to columns: 1 - Lagoa das Patas**,** 2 - Joe Lake, 3 - Camel Lake, 4 - Hanging Lake , 5 - Jack London L. , 6 - Jackson Pond, 7 - Cambará, 8 - Lake Patzcuaro, 9 - Rusaka Swamp, 10 - Lynches' Crater, 11 - Tierra del Fuego, 12 - Lake George, 13 - Potato Lake, 14 - Hay Lake.

Lag code	Location 1	2	3	4	5	6	7	8	9	10	11	12	13	14
1	+	+	+	+	+	+	+	+		−	−	−	−	−
2	+	+	+	+	+	−	+	+		−	−	−	−	−
3	+	+	+	+	+	−	+	+		−	−	−	−	−
4	+	+	+	+	+	−	+	+		−	−	−	−	−
5	+	+	+	+	+	−	+	**−**		−	−	−	−	−
6	+	+	+	+	+	−	+	−		−	−	−	−	−
7	+	+	+	+	+	−	+	−	+	−	−	−	−	−
8	+	+	+	+	+	−	+	−	**−**	−	−	−	−	−
9	+	+	+	+	+	−	+	−	−	−	−	−	−	−
10	+	+	+	+	+	−	+	−	−	−	−	−	−	−
11	+	+	+	**−**	+	−	+	−	−	−	−	−	−	−
12	+	+	**−**	−	+	+	+	−	−	−	+	−	−	−
13	+	**0**	**−**	**−**	**−**	+	+	**−**	**−**	**−**	+	**−**	**−**	**−**
14	+	0	−	−	−	+	**+**	−	−	−		−	−	−
15	+	0	**+**	−	−	+	+	−	−	−		−	−	−
16	+	0	+	−	−	**+**	+	−	−	−		−	−	−
17	+	0	+	−	−	+	+	−	−	−		−	−	−
18	+	0	+	−	−		+	−	+	−		−	−	−
19	**−**	0	+	−	−		+	−		−		−	−	−
20	−	0	**+**	−	**+**		**+**	−		−		−	−	−
21	−	0	+	−	+		+	−		−		−	−	−
22	−	0	+	−	**−**		+	−		−		−	−	−
23	−	0	+	−	−		+	−		−		−	−	−
24	−	0	+	−	−		+	−		−		−	−	**+**
25	−	0	+	−			+	**+**		−		−	−	+
26	**−**	0	+	**−**			+	+		**−**		**−**	**−**	+
27	−	**−**	+	−			+	+		−		−	−	+
28	−	−	+	−			+	+		−		−	−	**−**
29	−	−	+	**+**			+	+		−		−		+
30	**−**		**−**	+			+	+		**−**		**−**		+
31	−		−				+	+		−		−		**−**
32	−		−					+		−		−		−
33			**+**					**+**		−		−		−
34								+		−		−		
35										−		−		
36										−		−		
37										−		−		
38										−		−		
39										**−**		**−**		
40										−		−		

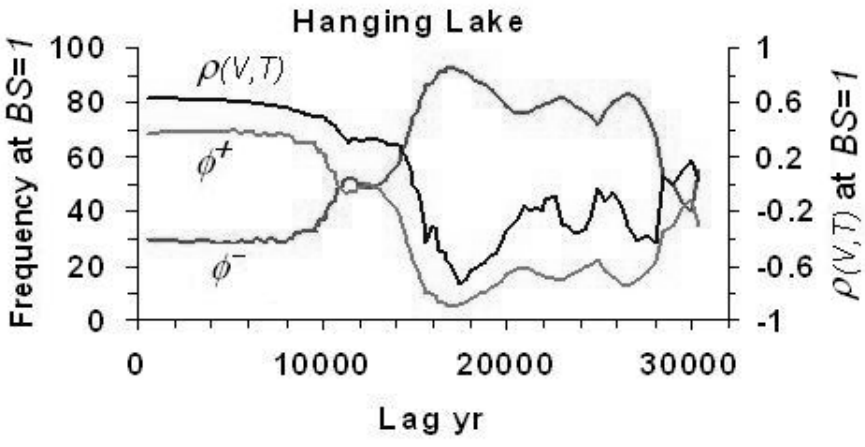

Figure 5. Lag dependent values of $\psi(V,T)$, λ^+ and λ^- graphed for the entire period in the Hanging Lake site. *Lag yr* indicated the number of years the temperature series is shifted to the left in Fig. 1 before reparing the *T* and *V* values. $\psi(V,T)$, λ^+ and λ^- are estimates at *BS* = 1. See main text, for method and comments.

Table 6. Hotspots detection based on peaks in compositional transition acceleration *(A* graphs) and extreme deviation from random expectation *(SSD*). Time points at which the extreme peaks occur are in *yr BP* columns. See definitions and discussion in the text.

Palynological sequence	Extreme *A*	*yr BP*	Extreme *SSD*	*yr BP*
Lagoa das Patas	0.00168	16380	35788; 23468	5523; 12122
Joe Lake	0.0211	10730	503291	10570
Camel Lake	0.511	11143	3617503	13040
Hanging Lake	0.179	9998	2592547	11287
Jack London L.	0.721; 1.908	9040;11980	$5.8x10^8$	12074
Jackson Pond	0.407; 0.373 ; 0.0276	58; 135;10673	87218	10857
Cambará	0.1; 0.1; 0262; 0.182; 0.00376	33; 673; 783; 928;19852	335173	12368
Lake Patzcuaro	0.00555; 0.00633	21476; 42759	20972	15396
Rusaka Swamp	0.0354; 0.0179; 1.208; 0.0217	1040; 7088; 9140;10280	492284; 294125	45513; 28210
Lynches Crater*	0.000154; 0.000114; 0.00142	14112; 118868; 164821	792587; 629056	900; 32732
Tierra del Fuego	0.394	9568	515049; 340976	12849; 10947
Lake George*	0.0261; 0.265	8470; 47411	47901238	34379
Potato Lake	0.0105; 0.00685	1471; 17641	1845477	17236
Hay Lake	0.159; 0.428; 0.169	2235; 19154; 42511	73725; 50529	42511;10003

*Current 40 k yr.

lynological composition; X_{ij} - a quantity of taxon *i* (pollen, spore, algal cell count) at time step *j*. A dot subscript indicates summation over the subscript that it replaces. We should mention that a zero X_{ij} will always have an associated D_{ij} value less than zero. We used *SSD* in the graphs of Fig. 3 and in Appendix 1. We construct the taxon specific graphs of D_{ij} (Fig. 6 and in Appendix 4). We are now ready to address the detection of hotspots and other characteristic points on the time axis.

Detection of hotspots and other characteristic points on the time axis

The indicator value of extreme peaks in the *A* graphs was mentioned, and the potential of the *SSD* graphs is obvious. The details are given in Table 6. Clearly, hotspot dating by locating extreme peaks on the *A* and *SSD* graphs is an analogue of edge detection (Orlóci and Orlóci 1990), in search of boundaries that separate qualitatively different segments within long ordered series.

We continue with considerations of specific aspects of the *V, A, SSD* and D^2 graphs in Fig. 6 and Appendix 4.

Hanging Lake. Observing the great age of the sediments, clearly, the site remained essentially unperturbed by glacial ice for at least forty millennia. The *V, A,* and *SSD* graphs (Fig. 3) remain flat and low close to the zero level during the period of dominant climate cooling. Low and flat graphs testify to a low intensity, highly stable palynological process. Then sharp oscillations begin to appear, heralding the advent of a period of intense dynamics, i.e., high instability. The changeover occurs in the wake of climate warming (sharp ascent of the *T* graph) and culminates around 11 k yr BP. Considering the *A* and *SSD* graph peaks, maximum compositional dynamics is registered after rapid temperature increase, ending more than 20,000 years of high stability. The sharp deviation peaks (Figure 6 and Appendix 4) of asco (Fu) and gonidium spore types (Pe) is an indication of the lichen element reaching maxima in the middle period. Earlier Fu and Pe do not deviate much from random expectation in stark contrast with the performance of cold steppe elements such as the Poaceae (Po), *Artemisia* (Ar), *Chenopodium* (Ch), and Brassicaceae (Br), the taxa that very much outperformed random expectation during the early period. The advent of the Holocene saw higher temperatures accompanied by increasing humidity. A most remarkable indicator of this episode is the peaking *Sphagnum* (Sp) around 5000 BP. By that time peat bog formation must have reached maximum extent in the region. The extreme peaks allow delimitation of the vegetation formations that moved through the Hanging Lake site over the millennia. The following identify the principal ecological indicator taxa and corresponding community habitat type for per time period:

∉ Up to 19400 – Poaceae, *Artemisia, Brassicaceae, Chenopodium*; shrub steppe on windswept dry uplands.

- 19,400 to 11,300 – *Pediastrum* (alga, lichen component), *Betula, Botrychium,* Fungi (lichen component), *Poaceae, Salix,* Cyperaceae, *Picea, Equisetum;* lichen dominated taiga, swamps expanding.
- 11,300 to 5,000 – *Alnus incana, Picea,* Ericales, *Vaccinium;* taiga uplands. *Sphagnum,* azonal peat bogs.
- After 5,000 – *Betula, Alnus,* Fungi, Cyperaceae, *Picea,* Ericales, *Vaccinium;* the taiga.

Cambará. We consider next the events that occurred during the same period at the Cambará site on the Atlantic rim of the Highlands in Rio Grande do Sul. We observe the major *SSD* peaks (Appendix 1) subdividing the vegetation process into 4 temporal phases. The densely arranged peaks indicate a period of intense dynamics, beginning around year 21500 BP just before the Vostok graph starts its steep ascent. Considering the taxon graphs in Appendix 4, deviation peaks of the hydrophytes, such as *Isoetes, Botryococcus*, and *Sphagnum* indicate increased regional humidity. Interesting to note the increased representation of *Isoetes* around 26000 BP, concomitant in time with the sustained decline of grasses (Poaceae). It is also interesting to note that *Isoetes* and the Poaceae reach bottom in negative deviation around 13000 yr BP when *Botrycoccus* attains maximum deviation. The *Sphagnum* peak around 759 BP indicates maximum peat bog formation in the site. *Araucaria* (Pinophyta) comes into considerable prominence around 759 BP in the wake of forest expansion over grassland, which was likely consequence of a more humid regional climate (Behling et al. 2004) coupled with the spatial process of expansion itself related to availability of dispersal agents and proximity of the site to forest seed sources (Duarte et al. 2006). *Araucaria* is seen reaching maximum deviation around 560 BP by which time the representation of Poaceae has fallen off considerably. *Araucaria* continuously outperforms random expectation until about 100 years ago from which point on its representation rapidly declines under the loggers' axe. The concurrent anthropogenic effect is tantamount to a complete redoing of the Highlands vegetation landscape. We refer to Behling et al. (2004) for other details. The Late Quaternary paleoecological history of Cambará can be read as the temporal march of life-zones over the site. The following identifies the principal eco-

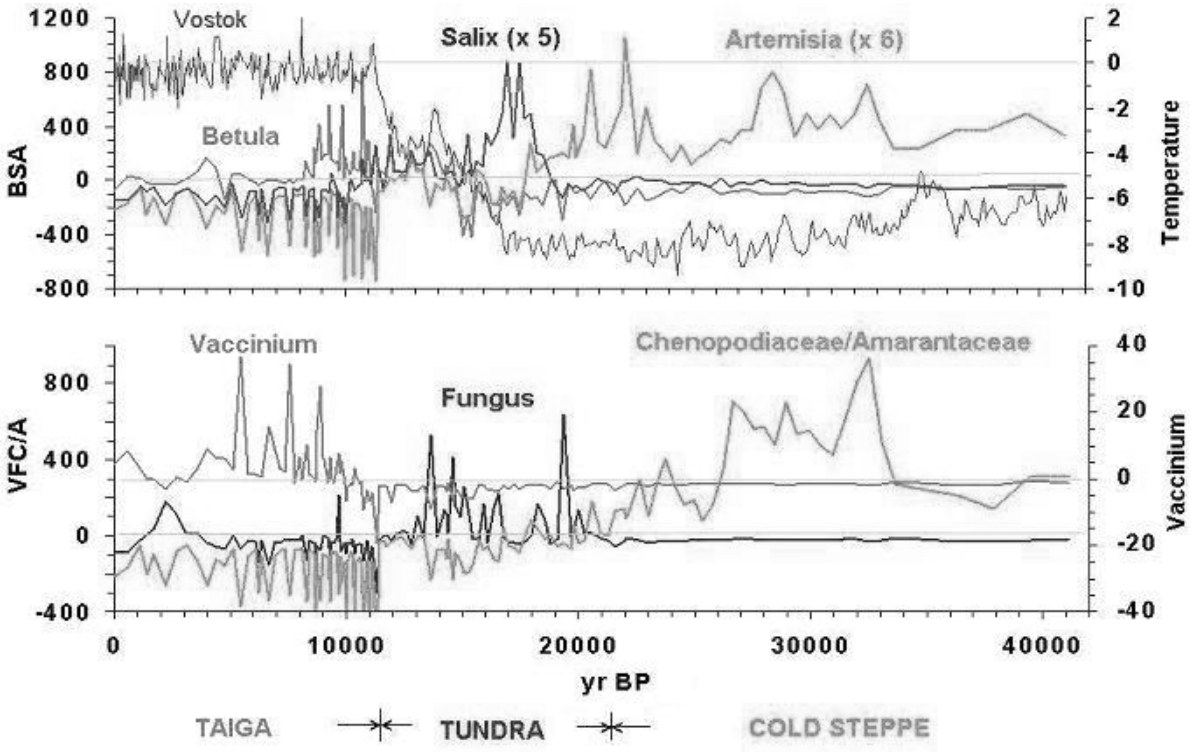

Figure 6. Vostok temperature *(T)* and deviation graphs for taxa as identified in Cwynar's Hanging Lake data set. Horizontal line across the graphs at zero is the base line for random expectation on the taxon scales and for temperature corresponding to current deuterium content on the Vostok scale. Deviations of taxa above or below the zero line indicate over or under-representation of those taxa in palynological collection, relative to expectation. *TBP* is time before present. The following percentages indicate proportions of the total sum of squared deviation *(SSD)* accounted for by the individual taxa in the total sample: *Betula* 19.1%, Fungus (ascospores) 8.5%; *Artemisia* 2.2%; *Sphagnum* 1.5%; *Salix* 0.9%; *Chenopodiaceae/Amaranthaceae* 0.1%; *Vaccinium* 0.01%. See method and references in the text.

logical indicator taxa and the community habitat type per time period:

- Up to 26,000 – Poaceae (zonal upland treeless Campos); *Myriophyllum* and *Isoetes*; azonal, shallow permanent ponds, mud flats.
- 26,000 to 11,500 – *Eryngium* (Apiaceae, a perennial semi-shrub), *Blechnum* (Blechnaceae) and *Poaceae*; zonal upland treeless Campos. *Botryococcus;* azonal mudflats; *Myriophyllum* and *Isoetes*; azonal, shallow permanent ponds.
- 11,500 to 758 – Poaceae, *Eryngium*; zonal upland Campos). *Sphagnum, Blechnum;* azonal peat bog. *Araucaria* increases and Poaceae decreases below expectation after 2000 BP.
- 758 to 100 – *Araucaria*; zonal treed upland. *Sphagnum*; blanket bog, peat bog.
- After 100 – Anthropogenic parkland, much of it under grazing. Reduced Poaceae and *Araucaria;* increased *Mimosa* and *Eryngium;* reduced *Sphagnum*.

The synchronicity results for V with the time shifted temperature series T can be used to find significant points at which a type of linkage to the past fades or changes direction considerably. These are the points where the serial lag-dependent (time shifted) graphs reach extreme points (Fig. 5, Appendix 3, Table 5) and the associated λ^+ and λ^- graphs come close together or even cross paths. We note that in the case of truncated cores, such as at Russaka Swamp, the Table 5 records should be referred back to the graphs in Fig. 5 and Appendix 3 for clarification.

Discussion

We begin by revisiting our reasons of the choices that determined the outcome. The decisions involve statistical technicalities and data aspects. We agree with those who warned us that the condition of the data, in the acquisition of which we had no control, could cast doubt on the paleoecological conclusions. But the methodology we introduce is different. It stands on its own internal logic and its suitability for the stated objectives.

Regarding the choice of palynological data, we preferred cases with long period length and rich lists of low-level taxa. Since the number of qualifying spectra is rather limited, the representation of the major vegetation formations is disproportionately heavier in the America's than on the other continents. This fact noted, we believe the 14 sites satisfy amply the requirement for a successful exposition of the power of our analytical approach. We mentioned reliability. In statistical analysis this will be eroded in proportion of the peculiar error properties of the data. We assume that sampling and measurement errors in the course of the original data acquisition do not exceed usual scientific standards. The choice to reach for a proxy model of long term atmospheric oscillations could not be avoided. We opted for the Vostok temperature records, relying on arguments put forward by us and others. Regarding the analysis, we can add to the arguments yet another point. This is our success to show linkages that certainly meet common sense expectation, which we consider as positive reflection back upon the suitability of the Vostok temperature oscillogram as a proxy for atmospheric temperature oscillations at the sites. The choice of transition scalars requires further comments:

1. Compositional transition velocity is proven, through the measurement of synchronicity, to be a reliable indicator of process sensitivity to environmental forcing. Ideally the synchronicity scalar should be partitioned according to the main effects, conditional effects, and interaction of several factors. But where should the data come from for this? We found long term records only for temperature.

2. Regularities found in velocity oscillations with regard to temperature oscillations indicate that global governing principles exist. But they do not indicate that these are exclusively climate related.

3. The significant departure of our results from random expectation on all levels almost in all the cases is an important, albeit not unexpected finding. Stated in other words, compositional transitions have levels of determinism and for that reason predictability, but never free of chance effects.

The general picture drawn about linkages of change in palynological composition and environment is a portrayal of tendencies played out in the past. The numerical results present interesting facts about these tendencies. Considering synchronicity and synchronicity scaling based estimation, and considering the determination of sign frequency distributions, the numerical results provide clarification of an important tendency: increasing atmospheric aridity (decreasing Thornthwaite index based on current evapotranspiration and precipitation rates) in tandem with decreasing values of λ^+. The statistical linkage shown could appear coincidental if it were not for the fact that the amplitude of environmental change at sites did not attain opposite extremes in aridity during the last 40 k yr. When the analysis is performed over a much longer period, such as in the case of Lynches' Crater, a different picture emerges. The 0 to 40 k yr BP period is dominated by λ^- and the 129 k to 190 k yr BP period is dominated by λ^+ as if a moister climate had existed earlier in that part of

Australia. To emphasize the climatic connection, it is interesting to mention the compositional change in the palynological spectrum after 129 k yr BP, highlighted by reduction in pollen counts of the Cunoniaceae (tropical trees), the lowland forest trees, the montane forest trees, the Cyatheae (tree ferns), and epiphytic Polypodiophyta, in contrast with the noted increase of *Agathis* (broad leaf conifer), Arecaceae (palms), dry forest trees and shrubs, and Poaceae which we found named in original records (Kershaw 1994). There are volumes of discussion about climate change in Australia during the last 200 k yr (Kershaw et al. 2002, Bowman 1998), but the details in that regard are outside the intended contents of this paper.

Compositional change, a permanent feature in the palynological spectra, at some points in time becomes extreme. The extreme points are indicated by spikes of acceleration *(A)* and deviations *(D)* from random expectation. We used Hanging Lake and Cambará as examples to illustrate this. The spikes clearly show extreme vegetation instability at the beginning of the current Interglacial from about 11 k yr BP until about 8 k yr BP. Maximum is reached around 10 k yr BP. The instabilities are climate related, but not necessarily uniquely climate defined.

Beyond local specificity, there is high-level coincidence in hotspots timing among the sites. Maxima around 10 k yr BP just after a steep millennial ascent of the Vostok temperature gradient, and again around 15 k yr BP and 20 k yr BP under similar settings is seen clearly in the graphs. Well defined hotspots occur in the immediate past at Jackson Pond (<200 yr BP), Cambará (<800 yr BP), and with one order of magnitude less intensity at Rusaka Swamp (<100 yr BP) and Potato Lake (<1500 yr BP). Increased frequency of fire and range wide cattle grazing have been shown specifically as major forcing events at Cambará (Behling et al. 2004). The extreme *A* and *SSD* peaks testify to the extraordinary destabilising effects of events since 800, most clearly human occupation in the last 100 years.

Hotspots occur within a roughly 3 k yr interval from 12 k yr BP at Jack London Lake, Camel Lake, and Harberton (Tierra del Fuego), and less intensely at Joe Lake and Hanging Lake. At Lynches Crater hotspots are most prominent during an earlier Ice Age cycle before 130 k yr BP. Based on period segments bounded by hot spots, we can trace the march of vegetation formations in the sites. We did this for Hanging Lake and Cambará. What can we read from these? The formations become destabilised after even short periods of warming. How long lasting is the effect? This and other specific questions are addressed in the final section.

Formation specificity of the processes associated with indicators λ^+ and λ^- are not well understood. One could point to water and temperature as limiting factors, assuming globally synchronous cooling and warming periods over the timeframe used and the resolution scale variable *(BS)*. One of the suggestions is that warming in humid zones speeds up the ecosystem processes and hence promotes vegetation change, while in atmospherically arid zones it does the opposite by aggravating water stress. Another suggestion is that changes in precipitation are inherently linked to changes in temperature (Wang et al. 2004), with opposite tendencies in the humid and arid zones: increasing the precipitation in the currently humid zones and decreasing it in the currently arid zones. It is true that fire history cannot be dismissed in arid zones as an influential factor, but as seen by Kershaw et al. (2002) it is difficult if not impossible to separate fire from climate. It makes sense to assume that climate change determines changes in fire regime. But anthropogenic ignition sources are important. The proposition that the time of the arrival of humans in a continent or island may be detected from aberrations in the λ^+ graphs appears confirmable.

Closing remarks

We return to our objectives and the objects of the core analysis: the *V* and *A* graphs; the synchronicity graphs computed from moving averages over *BS;* deviations graphs specific to *BS;* the graphs of ψ(V,T), λ^+ and λ^- at *BS* = 1 either as single values or as graphs. Now we will use what we so far presented to answer in brief specific questions we put about the palynological process:

Can the synchronicity of V and T be considered significant? Observe the 95% confidence limits in Table 3. Consider also that any estimate is deemed significant when the confidence limits do not enclose zero. Based on these conclude that compositional transitions have significant synchronicity with atmospheric temperature oscillation in all cases except one.

Are ψ(V,T), λ^+ and λ^- sensitively linked to the Thornthwaite Index? Observe ψ(V,T) Δ *Thi* = 0.621, λ^+ Δ *ThI* = 0.821, λ^- Δ *ThI* = 475?7; in Table 3 and conclude the presence of highly sensitive linkages.

Is synchronicity a current formation specific property of historic compositional transitions? Observe the distributions of λ^+ and λ^- in Tables 3 and 5 and the strong tendencies: dominance of λ^+ in the currently humid formations and same of λ^- in the currently arid formations. Conclude current formation specificity and conclude further a tendency of resistance against formation disintegra-

tion at levels of climate forcing characteristic in the Late Quaternary.

What about destabilisation? We interpret the previous tendencies as an indication that climate warming destabilises vegetation composition more readily in sites within the current climatically humid regions than in sites within the current climatically arid regions.

What about the temporal hotspots of change? The *A, SSD,* and *D* graphs presented reveal maximal transition dynamics in the wake of dramatic change in the environment. Climate warming and human activities figure as important triggers.

Does atmospheric temperature change have lasting effects on synchronicity? The evidence presented helps the reader to trace the serial correlation pattern of the *V* curve fixed in position and the *T* curve moved forward in time steps. Up to 10 k yr BP lag and in some cases much longer, there appears to be no change in frequency dominance relative to current formation type, except in the transitional cases which we already identified. How to interpret this? Dominance is a robust property of compositional change. To alter it, substantial forcing has to occur in the formation's climate. Our use of a minimum lag of 1 k yr should be considered further. At this minimum lag the observed stability in forward synchronicity is related to climate changes within the glacial cycle. For detecting whether synchronicity is stable at finer time scales, the minimum lag used in the analysis should be shorter, but then we would be limited by the time resolution constraint of the available data.

Acknowledgements. The authors received support from Conselho Nacional de Desenvolvimento Científico e Tecnológico (CNPq) and UFRGS of Brazil for L.O. and V.P.; The Natural Sciences and Engineering Council (NSERC) and Laurentian University of Canada for M.A. We acknowledge the data provider persons and institutions and thank the reviewers for constructive comments. Gratitude is expressed to M. Mihály for valued technical help.

References

Anderson, P.M. 1988. Late Quaternary pollen records from the Kobuk and Noatak River drainages, northwestern Alaska. *Quaternary Research* 29:263-276.

Anand, M. 2000. The fundamentals of vegetation change: complexity rules. *Acta Biotheoretica*. 48:1-14.

Anderson, R.S. 1993. A 35,000 year vegetation and climate history from Potato Lake, Mogollon Rim, Arizona. *Quaternary Research* 40:351-359.

Behling, H., Pillar, V. D., Orlóci, L. and Bauermann, S. G. 2004. Late Quaternary *Araucaria* forest, grassland Campos, fire and climate dynamics, studied by high-resolution pollen, charcoal and multivariate analysis of the Cambará do Sul core in southern Brazil. *Palaeogeography, Palaeoclimatology, Palaeoecology* 203:277-297.

Blunier, T. and Brook, E.J. 2001. Timing of millennial-scale climate change in Antarctica and Greenland during the Last Glacial Period. *Science* 291:109-112.

Bowman, D.M.J.S. 1998. The impact of Aboriginal landscape burning on the Australian biota. *New Phytol.* 140:385-410.

Bonnefille, R., Riollet, G., Buchet, G., Icole, M., Lafont, R., Arnold, M. and Jolly, D. 1995. Glacial/Interglacial record from intertropical Africa, high resolution pollen and carbon data at Rusaka, Burundi. *Quaternary Science Reviews* 14:917-936.

Clark, P.U., Pisias, N.G., Stocker, T.F. and Weaver, A.J. 2002. The role of the thermohaline circulation in abrupt climate change. *Nature* 415:852-859.

Colinvaux, P.A., de Oliveira, P.E. , Moreno, J.E., Miller, M.C. and Bush, M.B. 1996. A long pollen record from lowland Amazonia: forest and cooling in glacial times. *Science* 274:85-88.

Cwynar, L. C. 1982. A Late-Quaternary vegetation history from Hanging Lake, northern Yukon. *Ecological Monographs* 52:1-24.

Duarte, L. da S., Dos Santos, M.M.G., Hartz, S.M. and Pillar, V.D. 2006. The role of nurse plants on *Araucaria* forest expansion over grassland in South Brazil. *Austral. Ecology* (In Press)

Greig-Smith, P. 1952. The use of random and contiguous quadrats in the study of the structure of plant communities. *Ann. Bot.* 16:293-316.

Greig-Smith, P. 1983. *Quantitative Plant Ecology*. 3rd ed. Blackwell Scientific Publications, London.

Hannan, E.J. 1960. *Time Series Analysis.* Methuen, London.

IPCC. *Climate Change 2001: The Scientific Basis. Contribution of Working Group I to the Third Assessment Report of the Intergovernmental Panel on Climate Change*. Houghton, J.T., Ding, Y., Griggs, D.J., Noguer, M., van der Linden, P.J., Dai, X., Maskell, K. and Johnson, C.A. (eds.). Cambridge University Press, Cambridge, United Kingdom and New York, NY, USA, 2001. URL: http://www.ipcc.ch

Jacobs, B.F. 1985. A middle Wisconsin pollen record from Hay Lake, Arizona. *Quaternary Research* 24:121-130.

Kershaw, A.P. 1994. Pleistocene vegetation of the humid tropics of northeastern Queensland, Australia. *Palaeogeography, Palaeoclimatology and Palaeoecology* 109:399-412.

Kershaw, A.P., Clark, J.S., Gill, M.A., and D'Costa, D.M. 2002. A history of fire in Australia. In: Bradstock, R.A., Williams, J.E. and Gill, M.A. (eds), *Flammable Australia. The Fire Regimes and Biodiversity of a Continent.* Cambridge University Press, Cambridge, U.K. pp. 3-25.

Kühler, A.W. 1990. Natural vegetation. In: Espenchade Jr., E.B. and Morrison, J. L. (eds), *Rand McNally Good's World Atlas.* 18th edn. Rand McNally, New York. pp. 8-9.

Libby, W.F. 1955. *Radiocarbon Dating.* 2nd ed. University of Chicago Press, Chicago.

Lorius, C., Jouzel, J., Ritz, C., Merlivat, L., Barkov, N.I., Korotkevich, Y.S. and Kotlyahov, V.M. 1985. A 1500,000-year climatic record from Antarctic ice. *Nature* 316:591-596.

Lowe, J.J. and Walker, M.J.C. 1997. *Reconstructing Quaternary Environments.* 2nd ed. Longman, Harlow.

Lozhkin, A.V., Anderson, P.M., Eisner, W.R., Ravako, L.G., Hopkins, D.M., Brubaker, L.B., Colinvaux, P.A. and Miller, M.C. 1993. Late Quaternary lacustrine pollen records from southwestern Beringia. *Quaternary Research* 39:314-324.

Orlóci, L. 1993. The complexities and scenarios of ecosystem analysis. In: G.P. Patil and C.R. Rao (eds.), *Multivariate Environmental Statistics*. Elsevier Scientific, New York. pp. 423-432.

Orlóci, L. 1978. *Multivariate Analysis in Vegetation Research*. 2nd ed. W. Junk, The Hague.

Orlóci, L., Pillar, V.D., Anand, M. and Behling, H. 2002. Some interesting characteristics of the vegetation process. *Community Ecology* 3:125-146.

Orlóci, L. and M. Orlóci. 1990. Edge detection in vegetation: Jornada revisited. *Journal of Vegetation Science* 1:311-324.

Petit, J.R., Jouzel, J., Raynaud, D., Barkov, N.I., Barnola, J.-M., Basile, I., Bender, M, Chappellaz, J., Davisk, ,M., Delaygue, G., Delmotte, M., Kotlyakov, V.M., Legrand, M., Lipenkov, V.Y., Lorius, C., Pe´pin, L., Ritz, C., Saltzmank, E. and Stievenard, M. 1999. Climate and atmospheric history of the past 420,000 years from the Vostok Ice Core, Antarctica. *Nature* 300:429-436.

Petit, J.R. et al. 2000. *A Compendium of Data on Global Change. Carbon Dioxide Information Analysis Center*. Oak Ridge National Laboratory, U.S. Department of Energy, Oak Ridge, Tenn., U.S.A.

Petit, J.R., et al. 2001. *Vostok Ice Core Data for 420,000 Years*. IGBP PAGES/World Data Center for Paleoclimatology Data Contribution Series #2001-076. NOAA/NGDC Paleoclimatology Program, Boulder CO, USA.

Rayner, J.N. 1971. *An Introduction to Spectral Analysis*. Pion Limited, London.

Reynolds J.F, and Wu J. 1999. Do landscape structural and functional units exist? In: Tenhunen H.D. and Kabat P. (eds). *Integrating Hydrology, Ecosystem Dynamics, and Biochemistry in Complex Landscapes*, London: Wiley. pp. 273-296.

Ripley, B.D. 1977. Modelling spatial patterns. (With discussion.) *J. Royal Stat. Soc. Series B.* 39:172-212.

Ripley, B. D. 1981. *Spatial Statistics.* John Wiley, Chichester, UK.

Samuel, L., Foley, J.A., Brovkin, V. and Pollard, D. 1999. On the stability of the high-latitude climate-vegetation system in a coupled atmosphere-biosphere model. *Global Ecology and Biogeography* 8:489-500.

Schneider, D.C. 1994. *Quantitative Ecology: Spatial and Temporal Scaling.* Academic Press, San Diego.

Schweingruber, F.H. 1996. *Tree Rings and Environment Dendroecology*. Swiss Federal Institute for Forests Snow and Landscape Research, Birmensdorf and Paul Haupt, Bern.

Singh, G. and Geissler, E.A. 1985. Late Cainozoic history of vegetation, fire, lake levels and climate at Lake George, New South Wales, Australia. *Philosophical Transactions of the Royal Society of London Series B*, 311:379-447.

Stocker, T.F. 2000. Past and future reorganizations in the climate system. *Quaternary Science Reviews* 19:301-319.

Trewartha, G.T. 2001. Global Mechanism of UNCCD, Via del Serafico 107, 00142 Rome, Italy. Web address: www.gm-unccd.org/English/ Field/aridity.htm.

Trewartha, G. T. 1990. Climatic regions. In: Espenchade Jr., E.B. and Morrison, J.L. (eds), *Rand McNally Good's World Atlas*, 18th ed. Rand McNally, New York. pp. 8-9.

Walther, G. R., Post, E., Convey, P., Menzel, A., Parmesank, C., Beebee, T.J.C., Fromentin, J. M., Hoegh-Guldberg, O. and Bairlein, F. 2002. Ecological responses to recent climate change. *Nature* 416:389-395.

Wang, X., Auler, A.S., Lawrence Edwards, R., Cheng, H., Cristall, P.S., Smart, T. L., Richards, D.A. and Shen, C.-C. 2004 Wet periods in northeastern Brazil over the past 210 k yr linked to distant climate anomalies. *Nature* 432:740-743.

Watts, W.A. and Bradbury, J.P. 1982 Paleoecological studies at Lake Patzcuaro on the west-central Mexican Plateau and at Chalco in the Basin of Mexico. *Quaternary Research* 17:56-70.

Watts, W.A., Hansen, B.C.S. and Grimm, E.C. 1992. Camel Lake: A 40,000-yr record of vegetational and forest history from northwest Florida. *Ecology* 73:1056-1066.

Wilkins, G.R., Delcourt, P.A., Delcourt, H.R., Harrison, F.W. and Turner, M.R. 1991 Paleoecology of central Kentucky since the last glacial maximum. *Quaternary Research* 36:224-239.

Wiener, N. 1930. Generalized harmonic analysis. *Acta. math., Stockholm* 55:117-258.

Wonnacott, T.A. 1961. Spectral analysis combining a Bartlett window with an associated inner window. *Technometrics* 3:235-243.

Appendices

Downloadable from the web site of this issue at www.akademiai.com

Appendix EA7-1. Vostok temperature differences, compositional transition velocity, acceleration, and sums of squared compositional deviation from random expectation over time.

Appendix EA7-2. Graphical outline of the regression method for estimation of stable synchronicity and frequency values.

Appendix EA7-3. Lag-dependent synchronicity and sign frequency estimates.

Appendix EA7-4. Vostok temperature and taxon deviation graphs for taxa as identified in Cwynar's Hanging Lake and Behling's Cambará data sets.

Appendix EA7-5. Comments on results from calibrated and uncalibrated Cambará ages.

Received March 3, 2006
Accepted Apri 19, 2006

Appendix 1. Vostok temperature differences *(T),* compositional transition velocity *(V),* acceleration *(A),* and sums of squared compositional deviation *(SSD)* from random expectation over time (yr BP). Sites are presented in order as listed in Table 1. See Figure 3 as the model, details and references in the main text. Petit et al. (1999, 2000, 2001) present the temperature records. Time (horizontal axis) begins at the virtual top sediment horizon, missing in some of the records.

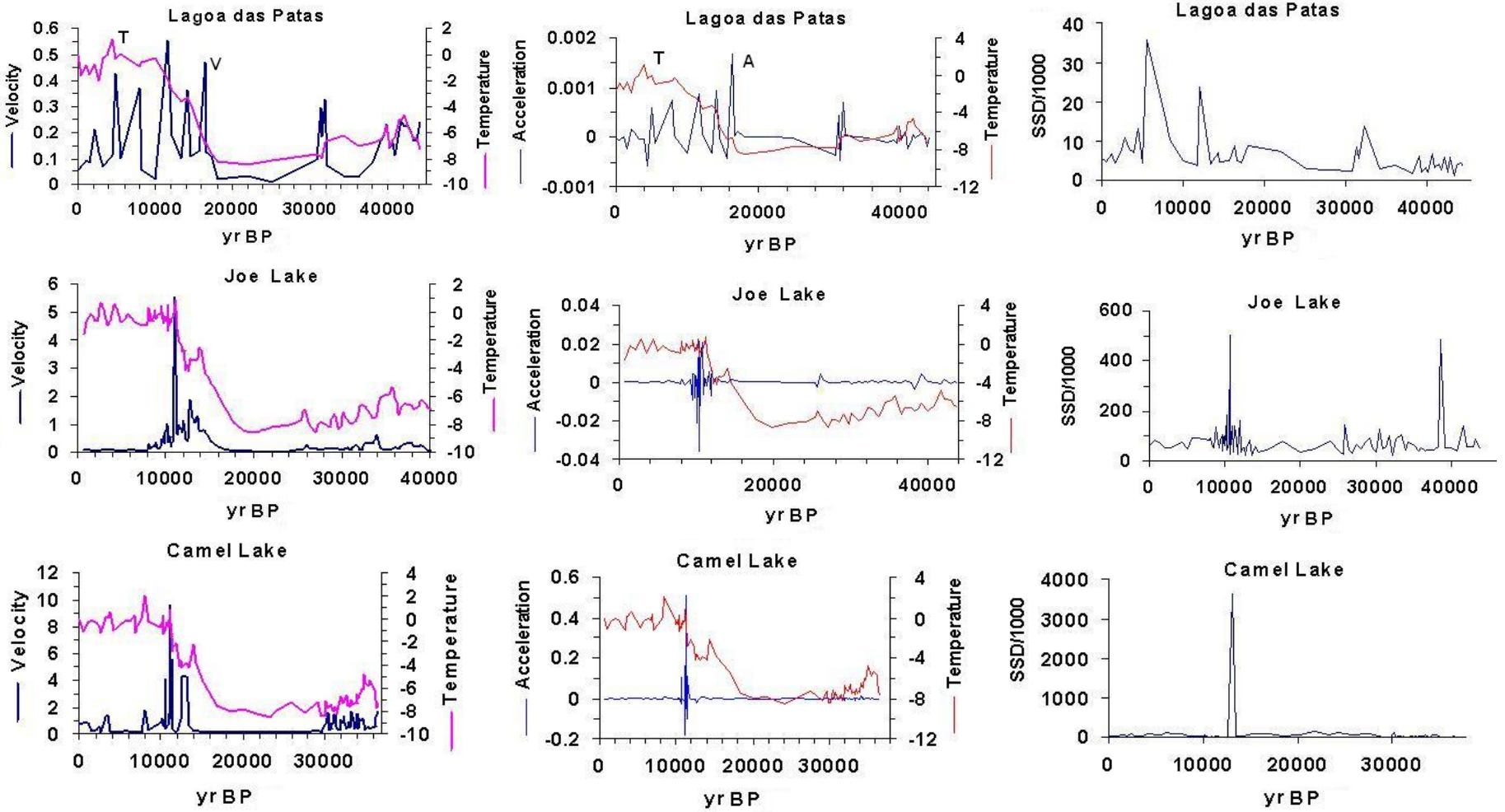

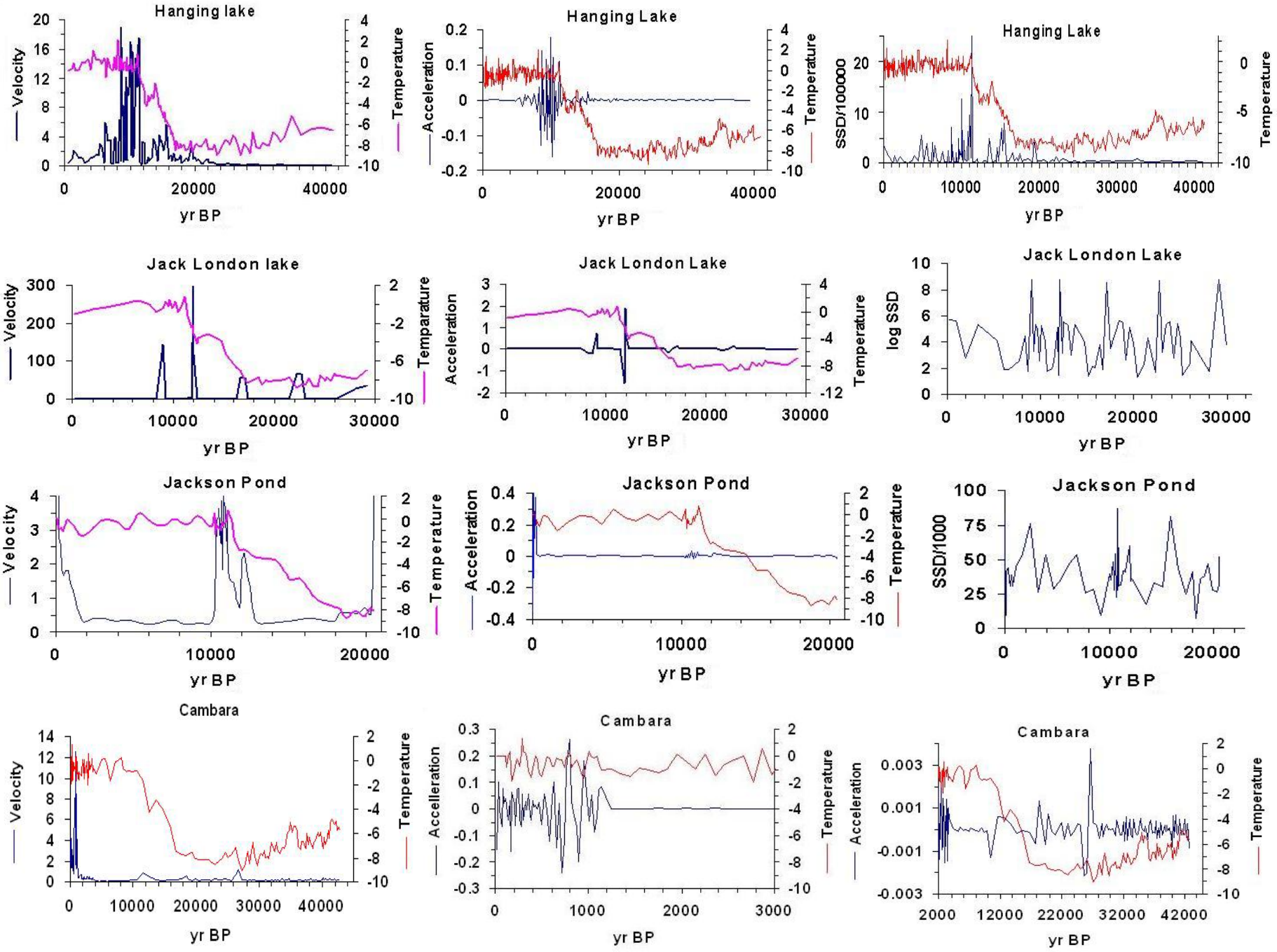
Hanging lake
Velocity
Temperature
yr BP
Hanging Lake
Acceleration
Temperature
yr BP
Hanging Lake
SSD/100000
Temperature
yr BP
Jack London lake
Velocity
Temparature
yr BP
Jack London Lake
Acceleration
Temperature
yr BP
Jack London Lake
log SSD
yr BP
Jackson Pond
Velocity
Temperature
yr BP
Jackson Pond
Acceleration
Temperature
yr BP
Jackson Pond
SSD/1000
yr BP
Cambara
Velocity
Temperature
yr BP
Cambara
Accelleration
Temperature
yr BP
Cambara
Acceleration
Temperature
yr BP

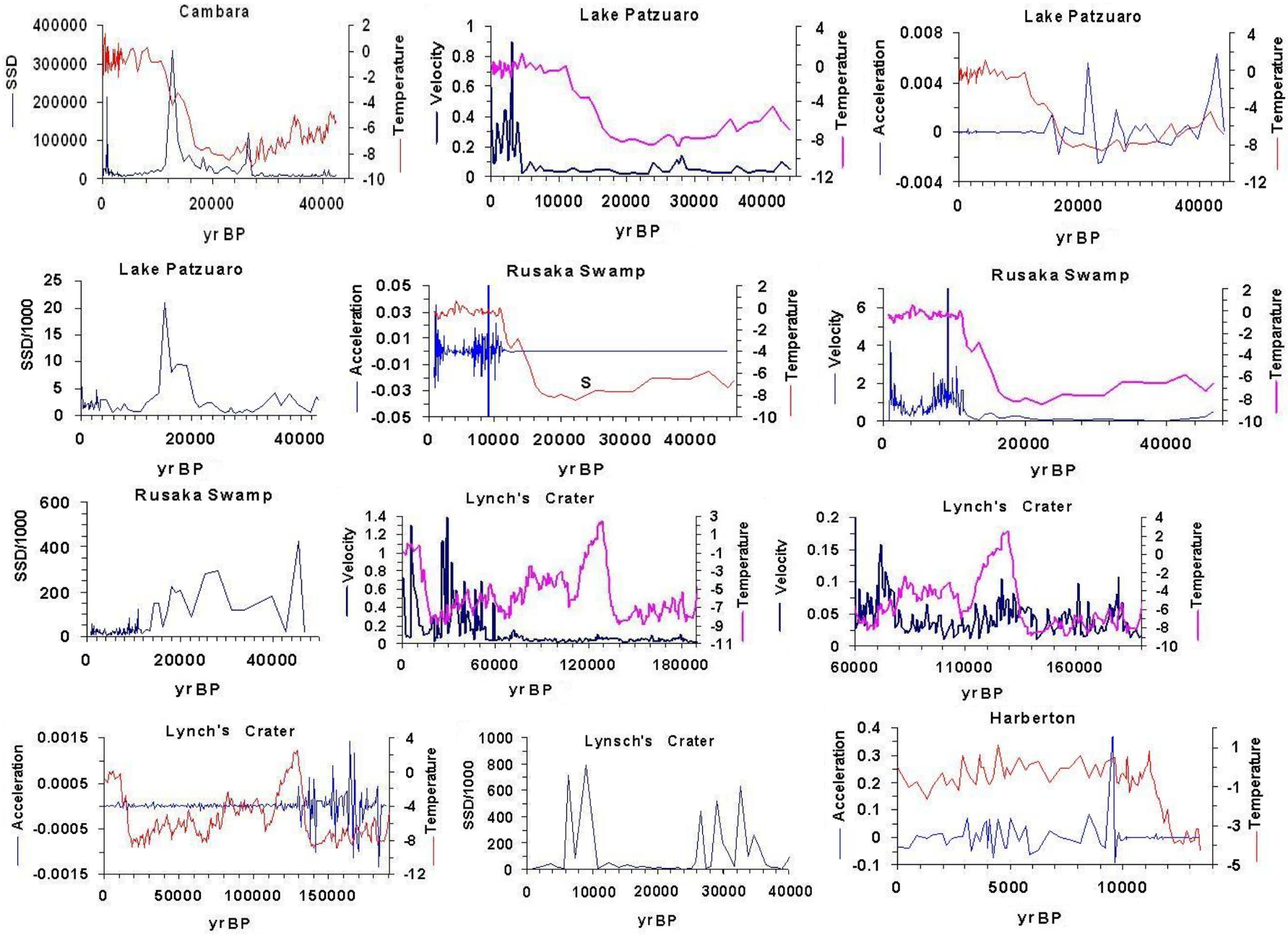
Cambara
SSD
Temperature
yr BP
Lake Patzuaro
Velocity
Temperature
yr BP
Lake Patzuaro
Acceleration
Temperature
yr BP
Lake Patzuaro
SSD/1000
yr BP
Rusaka Swamp
Acceleration
Temperature
S
yr BP
Rusaka Swamp
Velocity
Temparature
yr BP
Rusaka Swamp
SSD/1000
yr BP
Lynch's Crater
Velocity
Temperature
yr BP
Lynch's Crater
Velocity
Temperature
yr BP
Lynch's Crater
Acceleration
Temperature
yr BP
Lynsch's Crater
SSD/1000
yr BP
Harberton
Acceleration
Temperature
yr BP

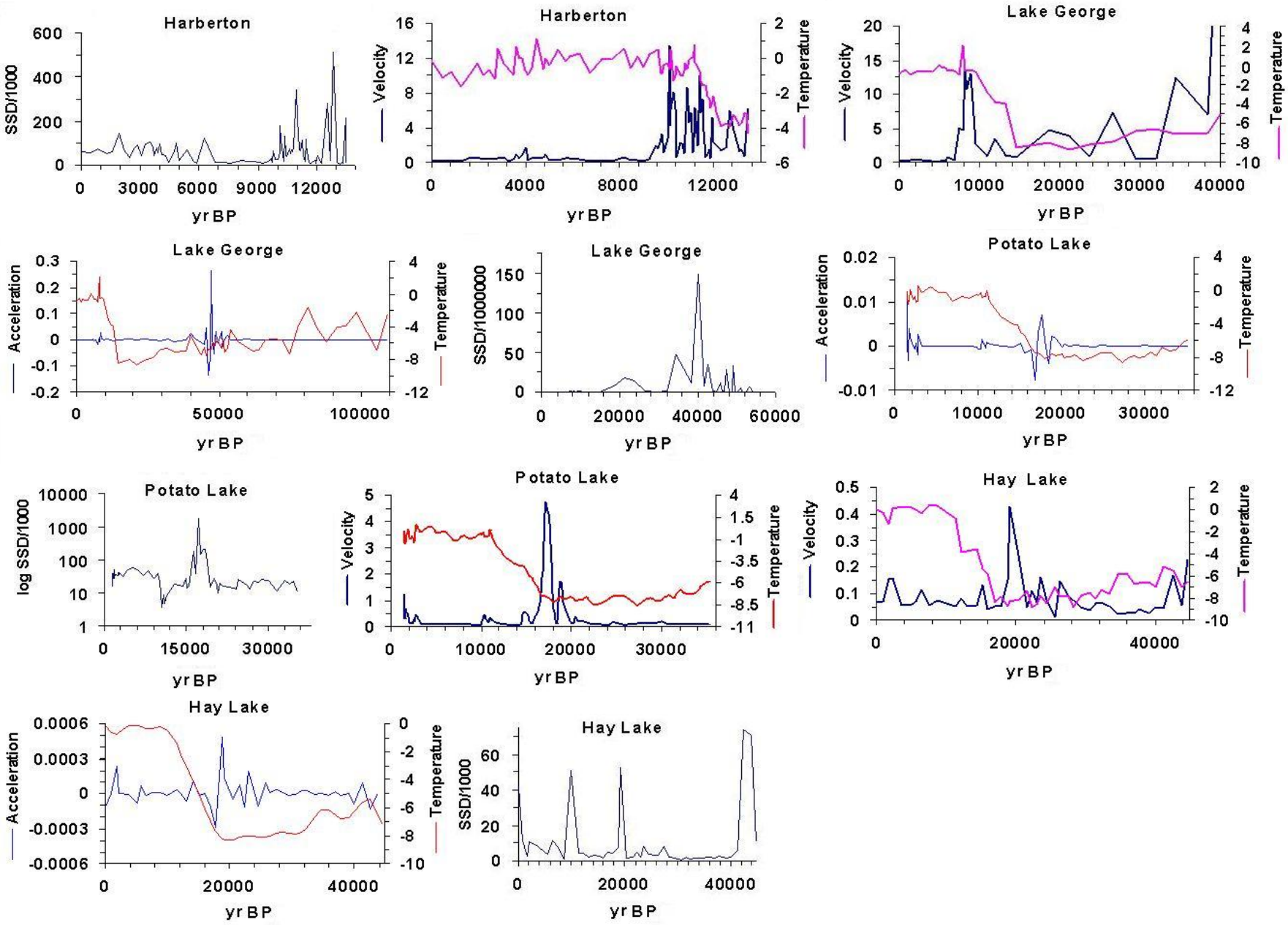
Harberton
SSD/1000
600
400
200
0
0 3000 6000 9000 12000
yr BP
Harberton
Velocity
Temperature
16
12
8
4
0
2
0
-2
-4
-6
0 4000 8000 12000
yr BP
Lake George
Velocity
Temperature
20
15
10
5
0
4
2
0
-2
-4
-6
-8
-10
0 10000 20000 30000 40000
yr BP
Lake George
Acceleration
Temperature
0.3
0.2
0.1
0
-0.1
-0.2
4
0
-4
-8
-12
0 50000 100000
yr BP
Lake George
SSD/1000000
150
100
50
0
0 20000 40000 60000
yr BP
Potato Lake
Acceleration
Temperature
0.02
0.01
0
-0.01
4
0
-4
-8
-12
0 10000 20000 30000
yr BP
Potato Lake
log SSD/1000
10000
1000
100
10
1
0 15000 30000
yr BP
Potato Lake
Velocity
Temperature
5
4
3
2
1
0
4
1.5
-1
-3.5
-6
-8.5
-11
0 10000 20000 30000
yr BP
Hay Lake
Velocity
Temperature
0.5
0.4
0.3
0.2
0.1
0
2
0
-2
-4
-6
-8
-10
0 20000 40000
yr BP
Hay Lake
Acceleration
Temperature
0.0006
0.0003
0
-0.0003
-0.0006
0
-2
-4
-6
-8
-10
0 20000 40000
yr BP
Hay Lake
SSD/1000
60
40
20
0
0 20000 40000
yr BP

Appendix 2. Graphical outline of the regression method for estimation of stable synchronicity and frequency values. Legend of symbols: *V* - compositional transition velocity; T - Vostok temperature; *BS* – block size for averaging; *r(V,T)* – synchronicity; F^+ and F^- - synchronicity sign frequencies; R^2 - coefficient of determination. See Figure 4 as model and explanations in the main text. Numerical results are summarised in Table 3. The values at *BS=1* are the stable estimates.

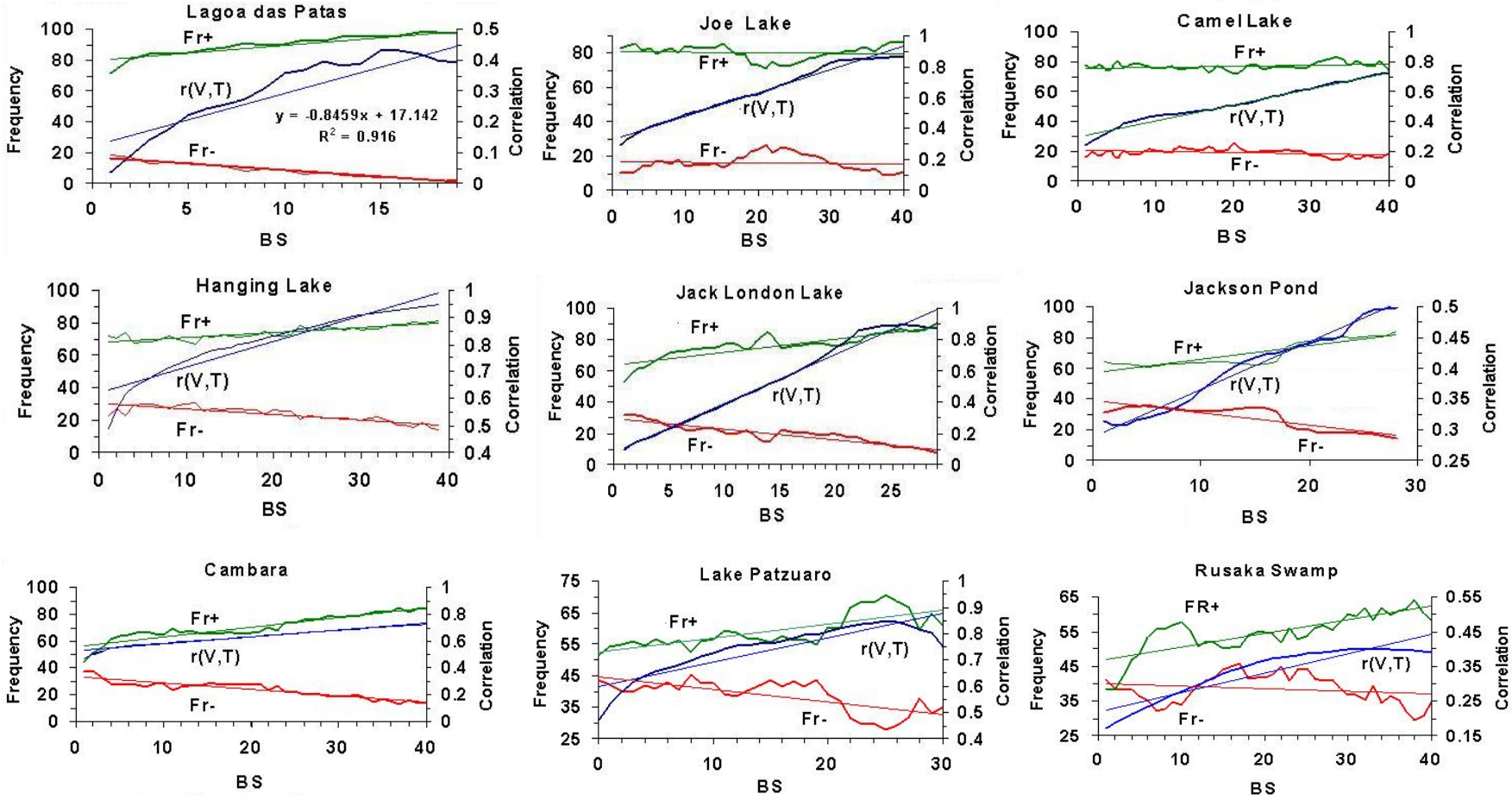

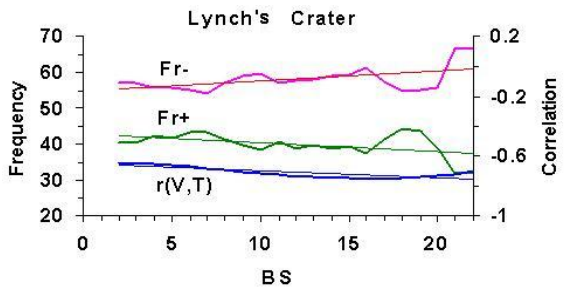
Lynch's Crater
Frequency
Correlation
Fr-
Fr+
r(V,T)
BS

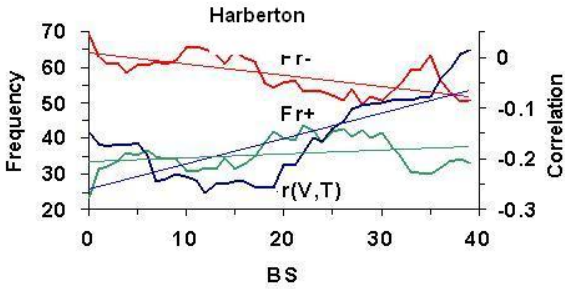
Harberton
Frequency
Correlation
Fr-
Fr+
r(V,T)
BS

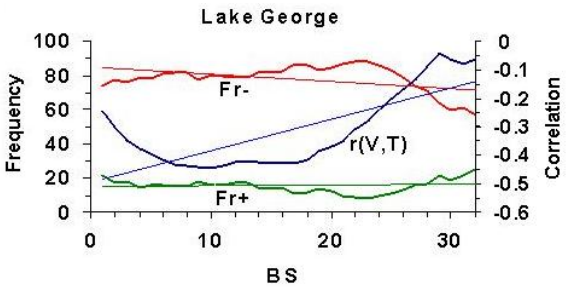
Lake George
Frequency
Correlation
Fr-
r(V,T)
Fr+
BS

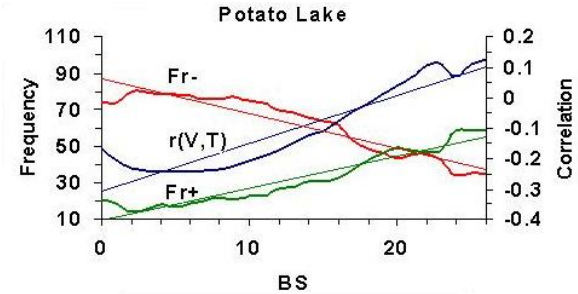
Potato Lake
Frequency
Correlation
Fr-
r(V,T)
Fr+
BS

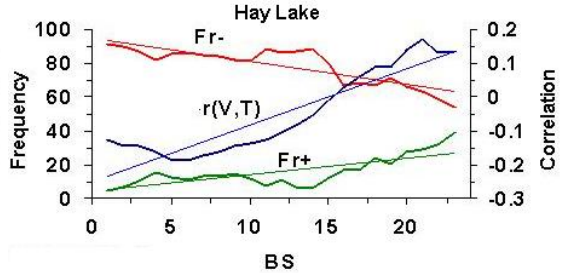
Hay Lake
Frequency
Correlation
Fr-
r(V,T)
Fr+
BS

Appendix 3. Lag-dependent synchronicity $\rho(V,T)$ and sign frequency estimates ϕ^+, ϕ^-. *Lag yr* indicates the number of years the temperature series is shifted to the left before re-pairing the *T* and *V* values. See Figure 5 in the main text as model and the explanations therein for interpretation of graphs. The graphs are presented in order of the locations listed in Table 1. All values graphed pertain to *BS=1.*

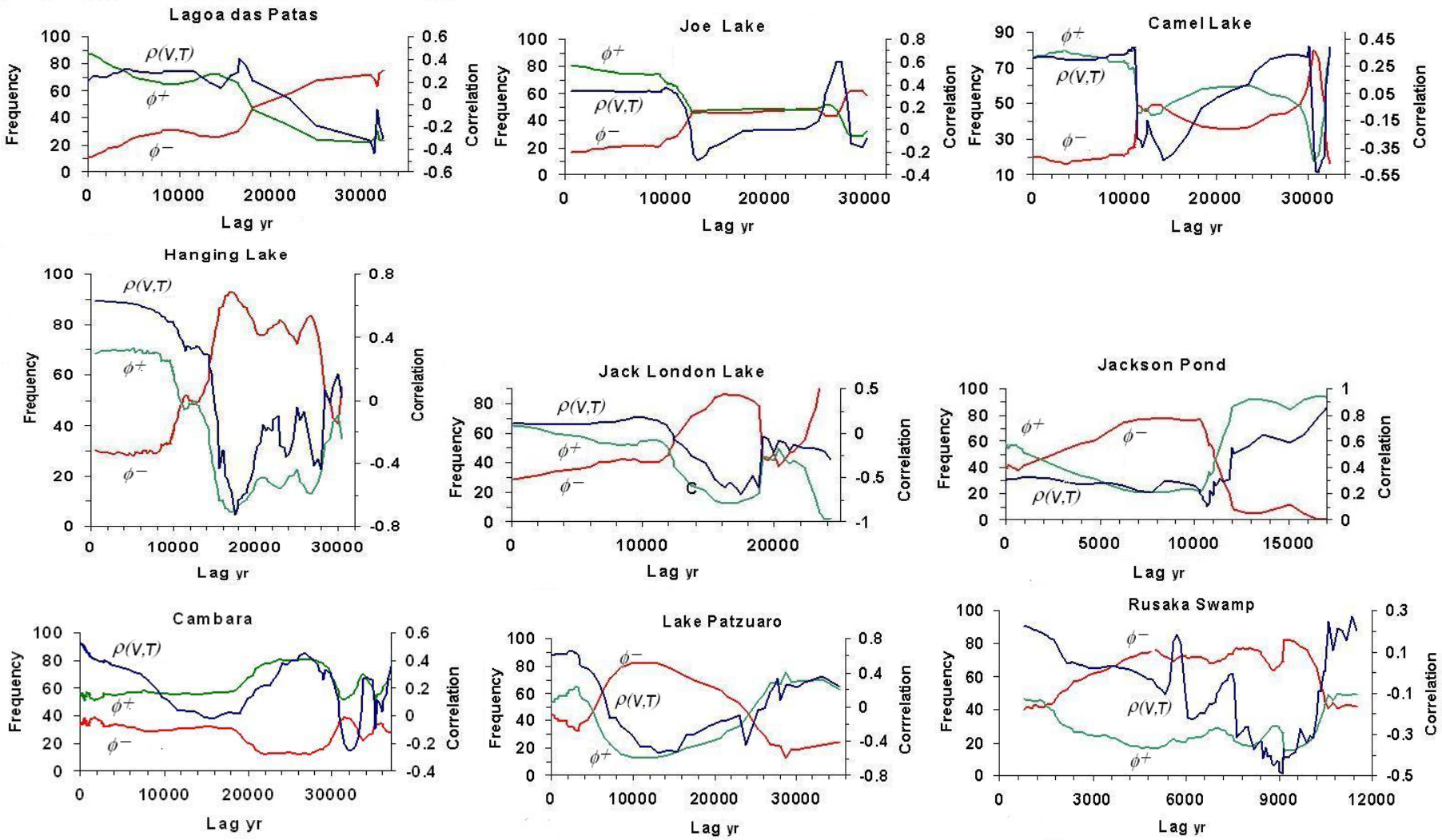

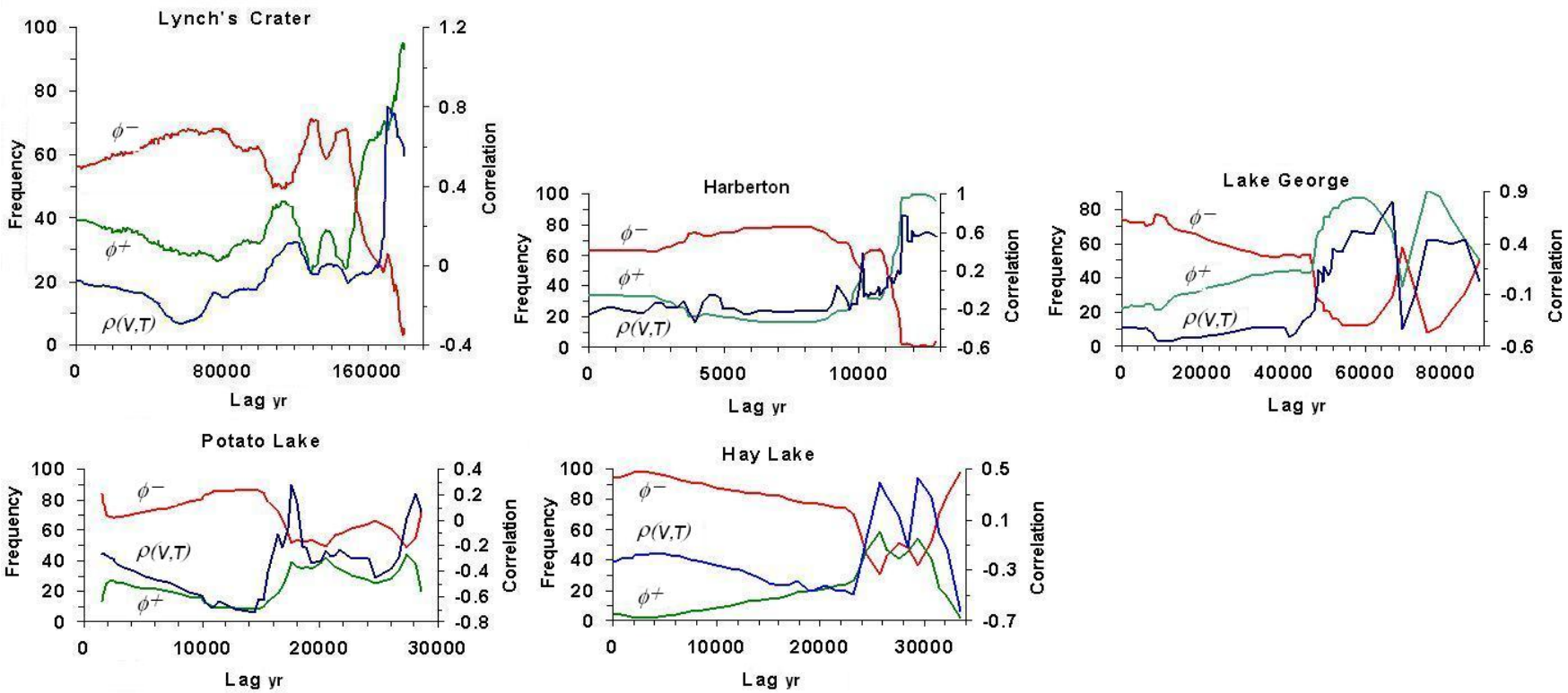
Lynch's Crater
Frequency
Correlation
Lag yr
ϕ^-
ϕ^+
$\rho(V,T)$
0
80000
160000
Harberton
0
5000
10000
Lake George
0
20000
40000
60000
80000
Potato Lake
0
10000
20000
30000
Hay Lake
0
10000
20000
30000

Appendix 4. Vostok temperature *(T)* and taxon deviation graphs *(D)* for taxa as identified in Cwynar's Hanging Lake (first 8 graphs) and Behling's Cambarà data sets. Horizontal line across the graphs at zero is the base line for random expectation on the taxon scales. Deviations of taxa above or below the zero line indicate over or under-representation in the palynological collection relative to expectation. See method and references in the main text. Locations are identified in Table 1. Use Figure 6 as model for interpretation. See explanation of the time scale *(yr B)* in the caption of Appendix 1.

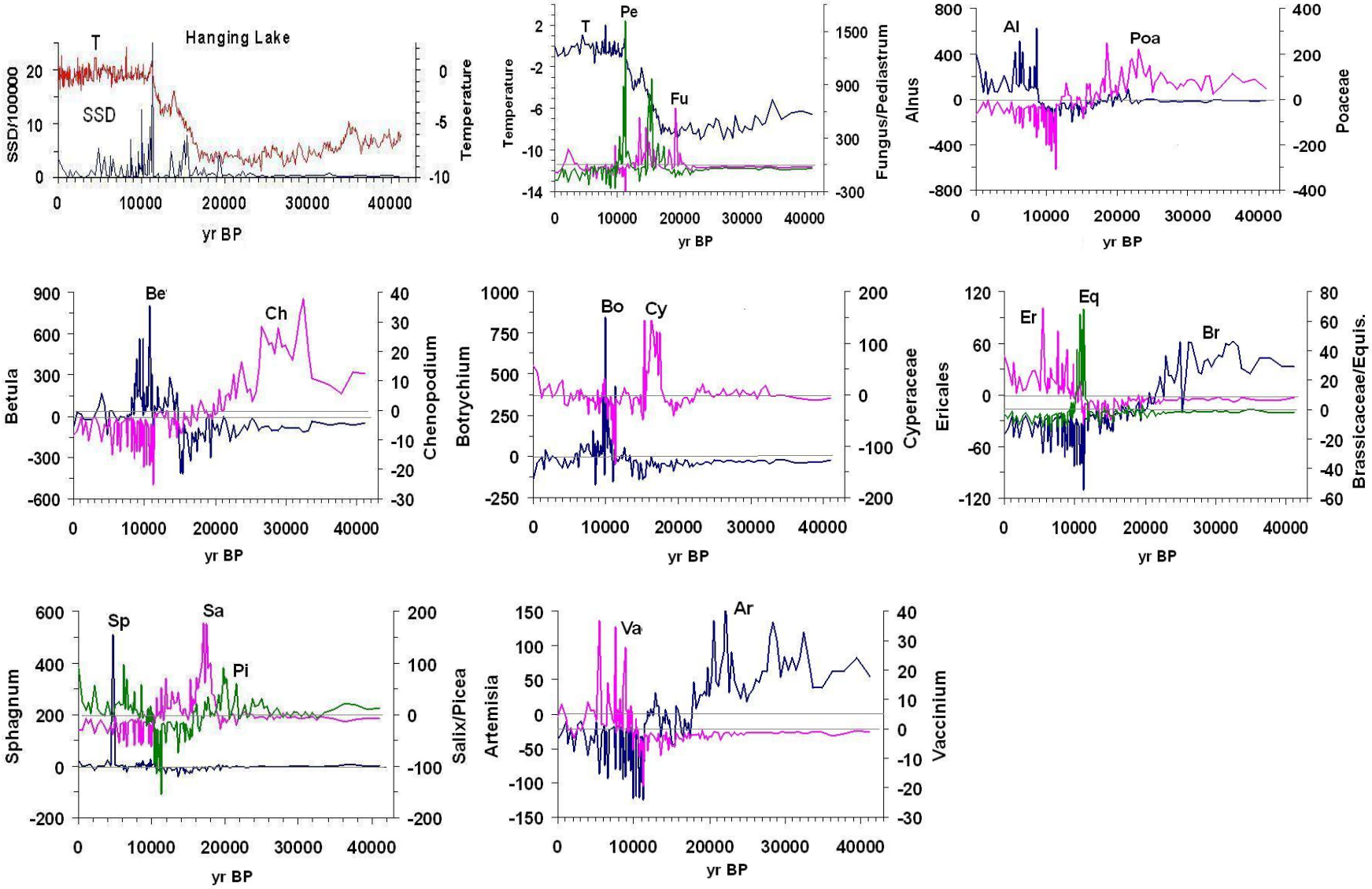

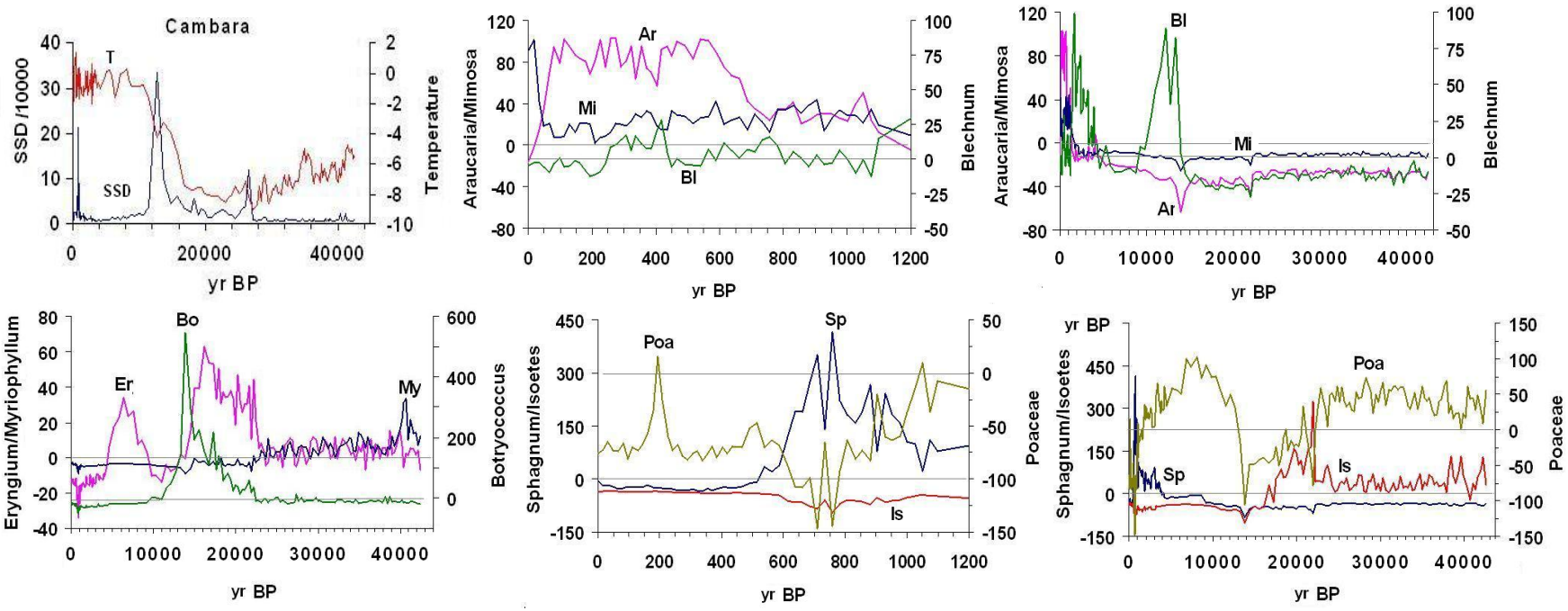
Cambara
SSD /10000
Temperature
T
SSD
yr BP
Araucaria/Mimosa
Blechnum
Ar
Mi
Bl
Eryngium/Myriophyllum
Botryococcus
Er
Bo
My
Sphagnum/Isoetes
Poaceae
Poa
Sp
Is

Appendix 5

Comments on results from calibrated and uncalibrated Cambarà ages

This discussion is based on the text in the Wikipedia web-based encyclopedia with our results added. According to the encyclopedia:

"Radiocarbon dating is based on the naturally occurring isotope carbon-14 to determine the age of carbonaceous materials up to ca 60,000 years. Within archaeology it is considered an absolute dating technique. The technique was discovered by Willard Frank Libby and his colleagues in 1949 (Libby, W. F.1985. *Radiocarbon Dating,* 2nd ed. Univ. of Chicago Press, Chicago)."

"The current maximum radiocarbon age limit lies in the range between 58,000 and 62,000 years. This limit is encountered when the radioactivity of the residual ^{14}C in a sample is too low to be distinguished from the background radiation."

"The raw radiocarbon dates, in BP years, are calibrated to give calendar dates. Standard calibration curves are available, based on comparison of radiocarbon dates of samples that can be independently dated by other methods such as examination of tree growth rings (dendrochronology), ice cores, deep ocean sediment cores, lake sediment varves, coral samples, and speleothems (cave deposits)."

H. Behling's data set (see Table 1 in the main text for details) includes both calibrated and uncalibrated age scales. We examined the scales in his data and found an almost perfect linear relationship between the calibrated and uncalibrated dates (Figure 7), and between the transition scalars *V, A* in linear correlation terms:

$r(V_{calbrated}, V_{uncaibrated})=0.996;\ \ r(A_{calbrated}, A_{uncaibrated})=0.991;\ \ r(Age_{calbrated}, Age_{uncaibrated})=0.995$

While we are aware of ambiguities with the linear correlation, we point out the cross plot of the velocity vales between the two age scales (Figure 8) as clear indication of an almost perfect linear relationship. But where a difference arose between the scales is the dating of hotspots. In all cases we relied on the uncalibrated scales. We mention the same conclusion for the synchronicity scalar *r(T,V)* as for *V*. The *SSD values* are time scale independent. See further comments in the main text.

Reference

Stuiver, M., P. J. Reimer and T. F. Braziunas. 1998. High-Precision Radiocarbon Age Calibration for Terrestrial and Marine Samples. Radiocarbon 40, 1127-1151.

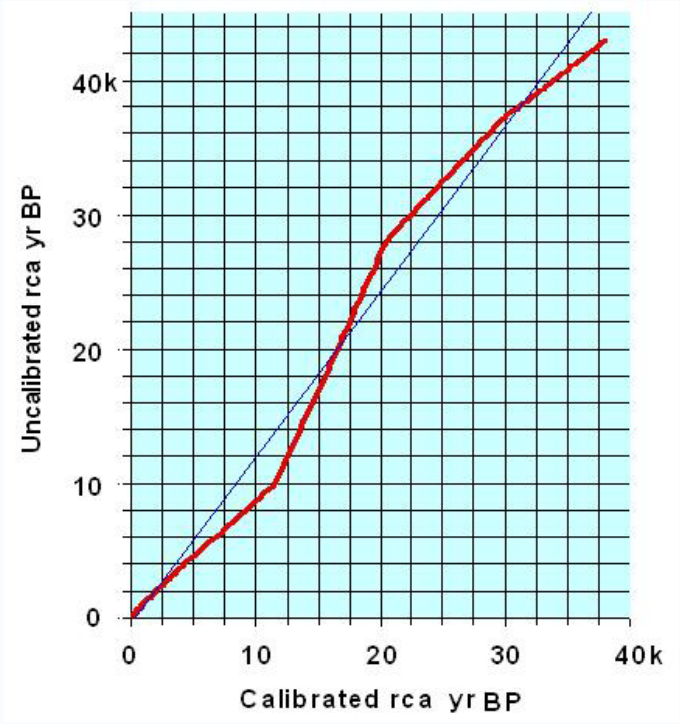

Figure 7. Behling's Cambarà calibrated and uncalibrated radiocarbon ages (rca) are compared. See data and site details Table 1 in the main text. Linear regression line is fitted to the observed line. The R^2 value of regression is *0.990.*

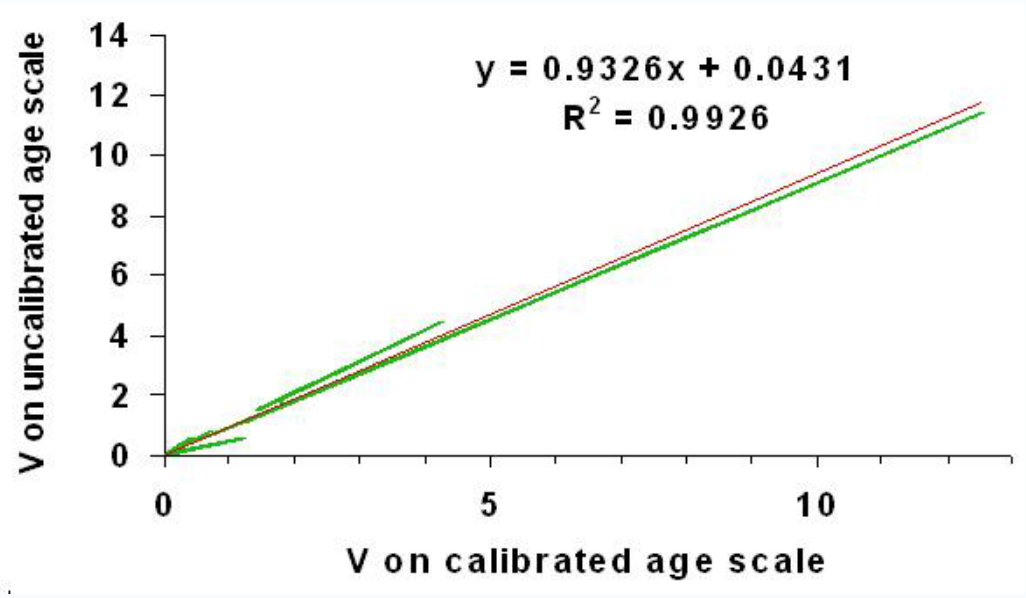

Figure 8. Cross plot of the velocity values between Behling's calibrated and uncalibrated age scales. Regression equation corresponds to fine line in centre. See the text for explanation.